NASA TECHNICAL NOTE

NASA TN D-3689

NASA TN D-3689

OPERATIONAL EXPERIENCE WITH THE ELECTRONIC FLIGHT CONTROL SYSTEMS OF A LUNAR-LANDING RESEARCH VEHICLE

by Calvin R. Jarvis

Flight Research Center
Edwards, Calif.

NATIONAL AERONAUTICS AND SPACE ADMINISTRATION • WASHINGTON, D. C. • OCTOBER 1966

NASA TN D-3689

OPERATIONAL EXPERIENCE WITH THE ELECTRONIC FLIGHT CONTROL SYSTEMS OF A LUNAR-LANDING RESEARCH VEHICLE

By Calvin R. Jarvis

Flight Research Center
Edwards, Calif.

NATIONAL AERONAUTICS AND SPACE ADMINISTRATION

For sale by the Clearinghouse for Federal Scientific and Technical Information
Springfield, Virginia 22151 – Price $2.00

OPERATIONAL EXPERIENCE WITH THE ELECTRONIC FLIGHT CONTROL SYSTEMS OF A LUNAR-LANDING RESEARCH VEHICLE

By Calvin R. Jarvis
Flight Research Center

SUMMARY

The electronic flight control systems of a free-flight lunar-landing research vehicle have enabled the craft to provide meaningful research information on pilot-controlled landings in a pseudolunar environment. The lunar-gravitational environment is effectively simulated by an electronic system and is accurate during hover and translation maneuvers to within 0.02 earth g. The attitude control system has proved to be effective and reliable in providing pilot control of vehicle attitude during all phases of operation investigated. The wide range of parameter variations provides a versatile control system for research investigations. The jet-engine attitude control systems have shown satisfactory response characteristics and excellent reliability. The lunar-simulation system has been effective in automatically controlling jet-engine thrust and attitude to provide a 1-lunar-g gravity vector acting on the vehicle and compensating for lift and drag aerodynamic disturbances.

Pilots have found that operation in a pseudolunar environment requires a markedly different control technique than is used in conventional vertical takeoff and landing (VTOL) operation. During lunar-simulation operations, the pilot is forced to lead the translational motions and to apply corrective attitude inputs early in order to decrease velocities over a prescribed marker. He must operate at much larger vehicle attitudes for longer durations than required for conventional VTOL operation.

The pilots found the use of motion and visual cues to be valuable in accomplishing translation maneuvers by vectoring the large jet-engine thrust in the gimbal-locked mode. For this reason, pilots indicated a preference for the gimbal-locked (VTOL) mode of operation over the local-vertical mode, which indicates that a more positive control of vehicle translation was possible with the gimbals locked.

INTRODUCTION

This nation's manned lunar-exploration program has fostered concentrated research in many areas. One of these areas is the definition of the numerous control requirements for accomplishing a pilot-controlled landing on the lunar surface. As a means of conducting research to define these requirements, the NASA Flight Research Center, at Edwards, Calif., procured and developed a free-flight vehicle to simulate lunar landings.

To simulate the lunar-gravity effect, the lunar-landing research vehicle, referred to as the LLRV, utilizes a vertically mounted jet engine to support five-sixths of the vehicle's weight. An electronic jet-engine attitude control system is used to automatically control the engine thrust and attitude, so that the engine remains essentially vertical with respect to the earth regardless of vehicle attitude. A "fly-by-wire," bang-bang vehicle attitude control system is used to provide manual control of vehicle attitude. During a lunar-simulation maneuver, one-sixth of the vehicle's weight is supported by a pair of lift rockets mounted on the main frame of the vehicle. Horizontal maneuvering and braking is accomplished by using the attitude rockets to control the outer frame and modulating the lift rockets, which are fixed to the frame.

Investigations related to the design of the free-flight lunar-landing research vehicle are discussed in references 1 and 2.

Two research vehicles were delivered to the NASA Flight Research Center in the spring of 1964. After delivery, several months were devoted to checking systems and installing research instrumentation. During this period, many problems were encountered which required extensive modifications to the vehicle and its systems. Subsequent development flight testing disclosed additional problems and resulted in further modifications. This paper discusses the nature of these problems and the performance of the flight control systems during the early flights.

SYMBOLS

Measurements for this investigation were taken in U. S. Customary Units, and equivalent values are indicated herein in the International System of Units (SI). Details concerning the use of SI, together with physical constants and conversion factors, are given in reference 3.

A, B, C, D, E, F, G, H	attitude-rocket notation
f	frequency, cycles per second
g	acceleration due to earth's gravity, 32.2 feet per second^2 (9.80 meters per second^2)
h	altitude, feet (meters)
K	amplifier gain
m	vehicle mass, slugs (kilograms)
s	Laplace operator
T	thrust, pounds (newtons)
$\frac{T}{W}$	ratio of thrust acting on vehicle to vehicle weight
t	time, seconds

W	vehicle weight, pounds (newtons)
x,y,z	earth-reference positions, feet (meters)
$\ddot{x}$	longitudinal acceleration, feet per second^2 (meters per second^2)
$\ddot{y}$	lateral acceleration, feet per second^2 (meters per second^2)
$\ddot{z}$	normal acceleration, feet per second^2 (meters per second^2)
Δ	incremental change
ζ	damping ratio
Θ	pitch angle, degrees (radians)
φ	roll angle, degrees (radians)
$\dot{\psi}$	yaw rate, degrees per second (radians per second)
ω_n	natural frequency, cycles per second

Subscripts:

b	body axis
c	command input
g	gimbal
i	initial value
j	jet engine
lr	lift rocket
S	standard
T	test
v	vehicle

BRIEF DESCRIPTION OF THE LLRV FLIGHT CONTROL SYSTEMS

A detailed description of the vehicle and associated hardware is presented in reference 4. Figures 1(a) and 1(b) show the LLRV on the ground and in flight, respectively.

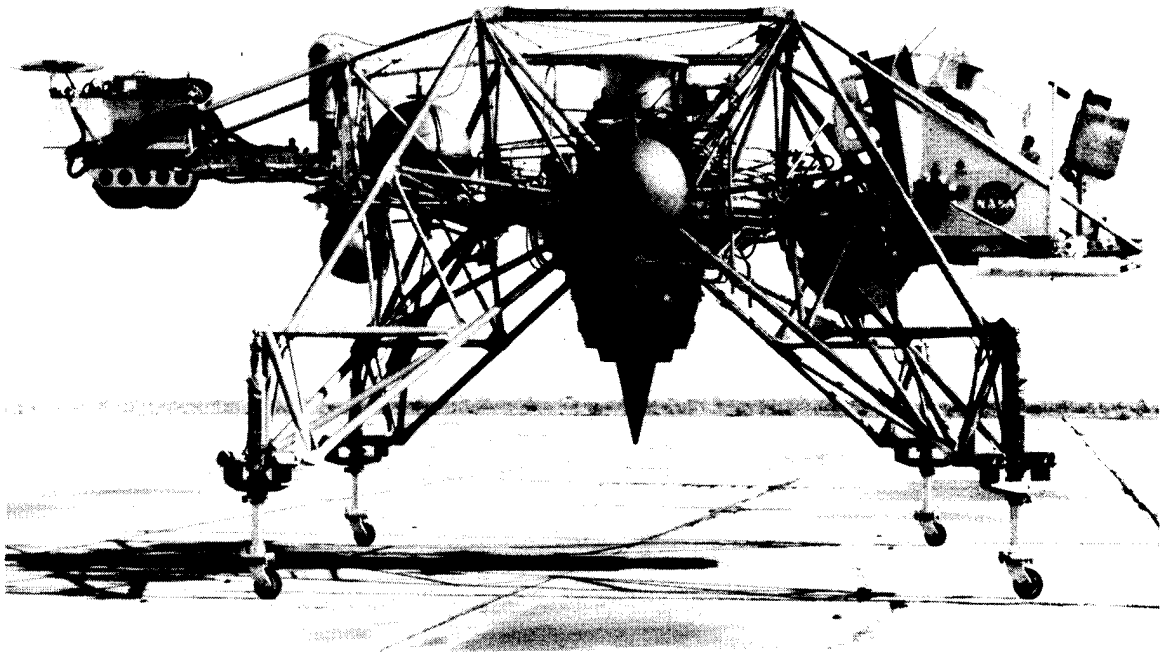

E-12318

(a) On the ground.

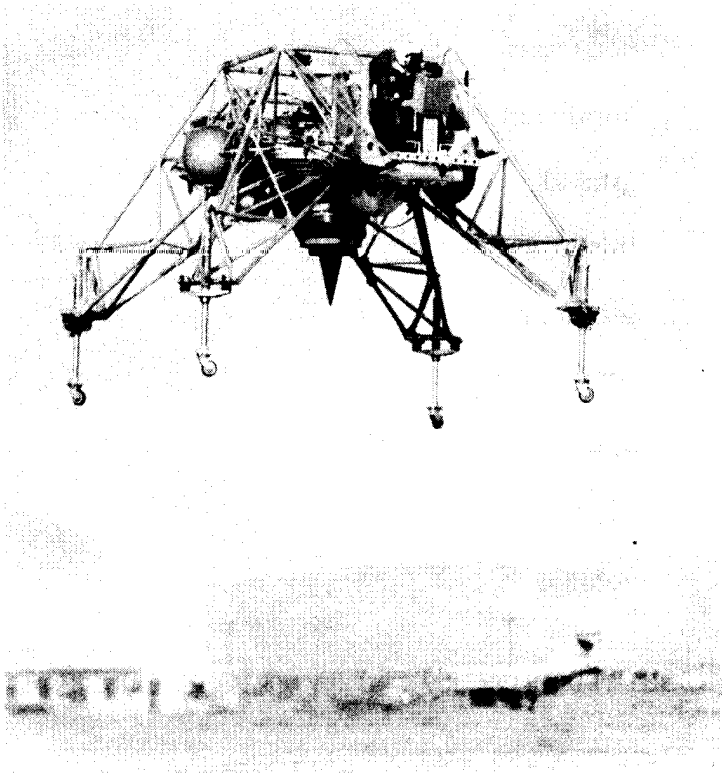

ECN-543

(b) In flight.

Figure 1.– The lunar-landing research vehicle.

Basically, the vehicle consists of a four-leg tubular framework extending from a lightweight central structural-ring assembly. The ring assembly accommodates a vertically mounted jet engine through large pitch and roll gimbals. Eight 500-pound-thrust (2225 newtons) hydrogen-peroxide lift rockets are mounted to the structural-ring assembly. Two of the rockets provide lift thrust during lunar-simulation operation. The remaining six are used for vehicle recovery in the event of jet-engine failure. The pilot operates the lift rockets with a collective stick arrangement attached near the floor of the cockpit and to the left of the seat. The pilot's cockpit is located between the two forward legs of the vehicle. The platform assembly, mounted between and extending aft of the two rear legs, contains the electronic hardware.

Figure 2 shows the various electronic assemblies that make up the LLRV flight control systems. The electronic hardware associated with each system was originally designed to be self-contained in separate assemblies for maintenance convenience and quick turnaround substitution in the event of malfunctions.

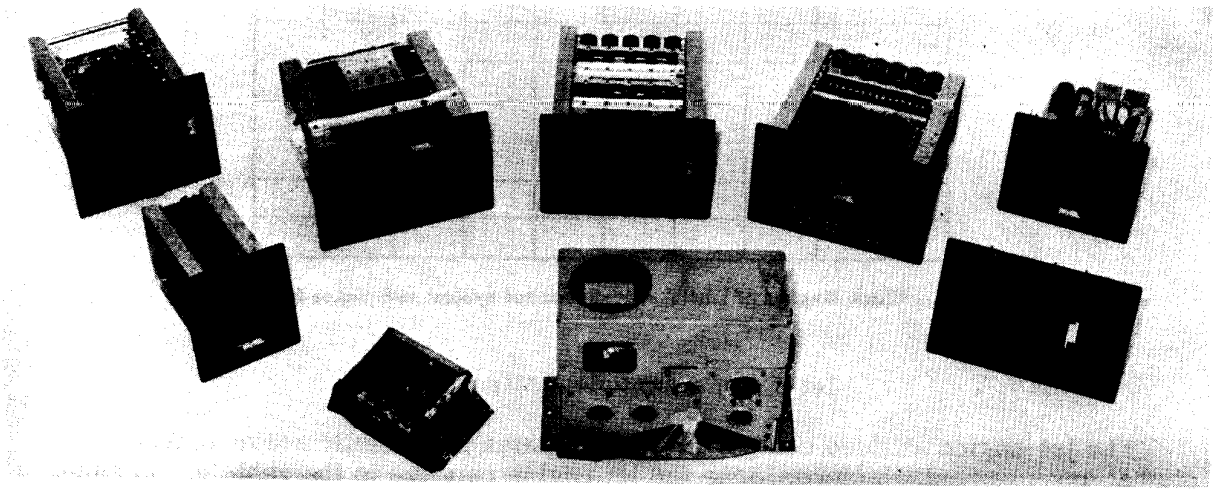

E-14322

Figure 2.– LLRV electronic flight control system hardware.

Attitude Control System

The LLRV attitude control system (ACS) is a bang-bang, fly-by-wire system capable of operating in either attitude command, rate command, or acceleration command modes. A conventional center stick is used for pitch and roll control and rudder pedals for yaw control. Two separate sets of attitude rockets are used for attitude control. The designations for each rocket, the associated moment arms, and the firing logic are shown in figure 3. The attitude rockets were designed to be operated in an on-off manner with a fixed, but ground adjustable, thrust range of 18 pounds (80 newtons) to 90 pounds (400 newtons). The desired thrust is obtained by adjusting propellant flow to the individual rockets. The system circuitry and operation is discussed in detail in appendix A.

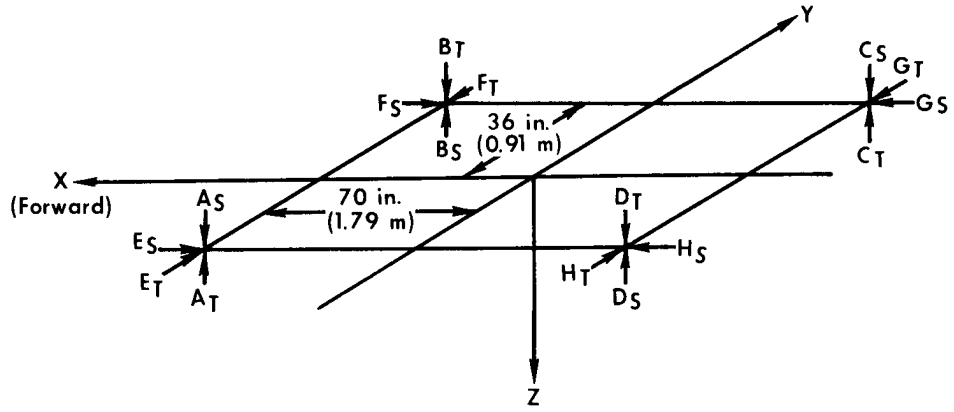

Rockets with subscript S denote standard rockets fire.
Rockets with subscript T denote test rockets fire.
For dual-system operation, both standard and test rockets fire.

Rocket	A_S A_T	B_S B_T	C_S C_T	D_S D_T	E_S E_T	F_S F_T	G_S G_T	H_S H_T
Pitch Up	✓	✓	✓	✓				
Pitch Down	✓	✓	✓	✓				
Roll Right	✓	✓	✓	✓				
Roll Left	✓	✓	✓	✓				
Yaw Right					✓	✓	✓	✓
Yaw Left					✓	✓	✓	✓
Pitch up and roll right	✓		✓					
Pitch up and roll left		✓		✓				
Pitch down and roll right		✓		✓				
Pitch down and roll left	✓		✓					

Figure 3.– Block diagram of LLRV attitude control system and rocket-firing logic.

Jet-Engine Attitude Control System

The jet-engine attitude control system operates a hydraulic servo-driven dual-gimbal arrangement which positions the jet engine relative to the vehicle. In addition to lunar-simulation operation, the system may be operated in any of three different modes: local-vertical, engine-centered, and gimbal-locked. In the local-vertical or engine-centered modes of operation, the attitude of the jet engine is controlled electrically. The gimbal-locked mode is a hydraulic lock mechanism designed for emergency use in the event of a failure of the electrical systems. Indicator lights on the instrument panel show the status of the systems during flight. Separate switches are used for engaging and disengaging the local-vertical and gimbal-locked modes. The engine-centered mode is automatically selected when the local-vertical and gimbal-locked switches are in the off position. The operation of the jet-engine attitude control subsystems is described in detail in appendix B.

Lunar-Simulation System

The LLRV lunar-simulation system controls the jet-engine attitude and throttle position so that five-sixths of the vehicle's weight is canceled by the jet thrust. The system also automatically compensates for measurable acceleration changes resulting from aerodynamic disturbances such as lift and drag. The system (fig. 4) consists of

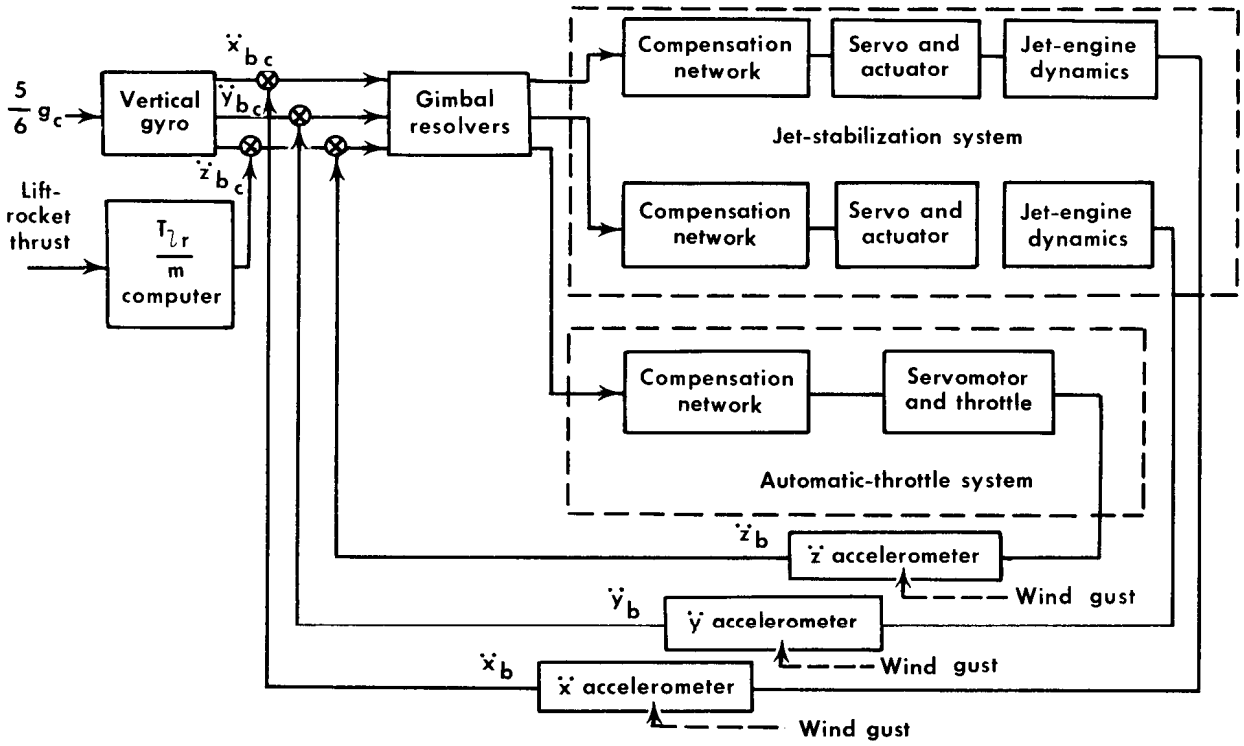

Figure 4.– Simplified block diagram of the LLRV lunar-simulation system.

two separate subsystems: the jet-stabilization system (JSS) and the automatic-throttle system (ATS). The JSS controls the jet-engine pitch- and roll-gimbal position to compensate for aerodynamic disturbances. The ATS automatically controls the jet-engine thrust for the five-sixths vehicle-weight compensation.

Also incorporated in the lunar-simulation system is a thrust-to-weight $\left(\frac{T_{lr}}{W}\right)$ computer that determines the initial weight of the vehicle when the system is activated and computes the acceleration of the vehicle resulting from lift-rocket operation during a lunar-simulation maneuver. The computer is also mechanized to compensate for the change in vehicle mass resulting from fuel burnoff.

The lunar-simulation system and associated subsystems are described in detail in appendix C.

SYSTEM DEVELOPMENT PROBLEMS

Structural Vibration

During initial closed-loop tests of the LLRV control systems, several instabilities occurred as the result of coupling with vehicle structural modes. The lightweight construction of the framework and gimbals resulted in several low-frequency vibration modes which were within the operational bandwidths of the flight control systems.

Jet-engine attitude control system. – The effect of structural vibrations on the response of the jet-engine attitude system is illustrated in figure 5, a time history of

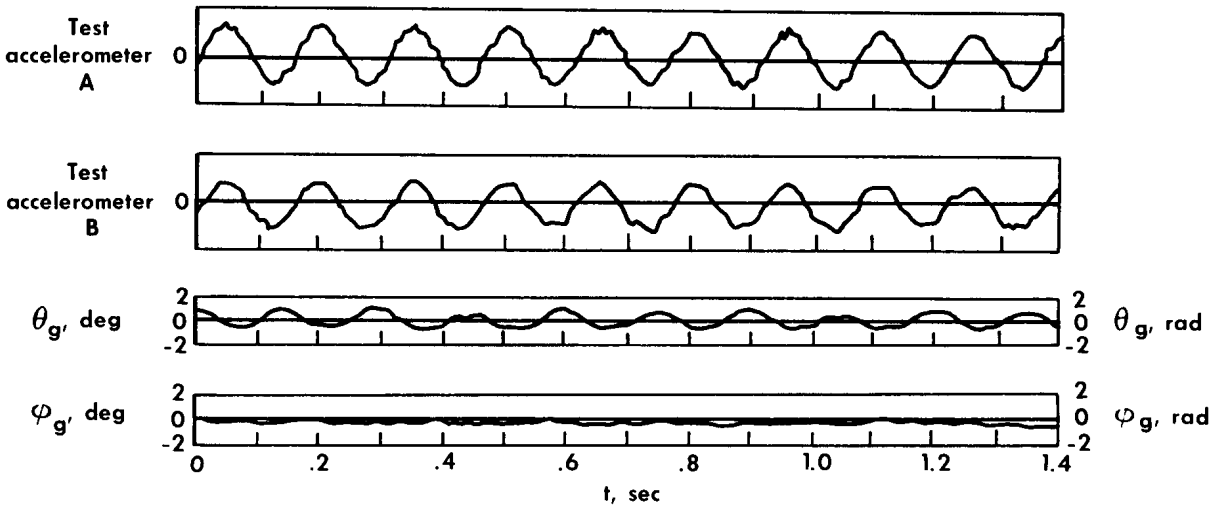

Figure 5.– Sustained oscillation of the jet-engine attitude system resulting from a 6.7-cps structural resonance.

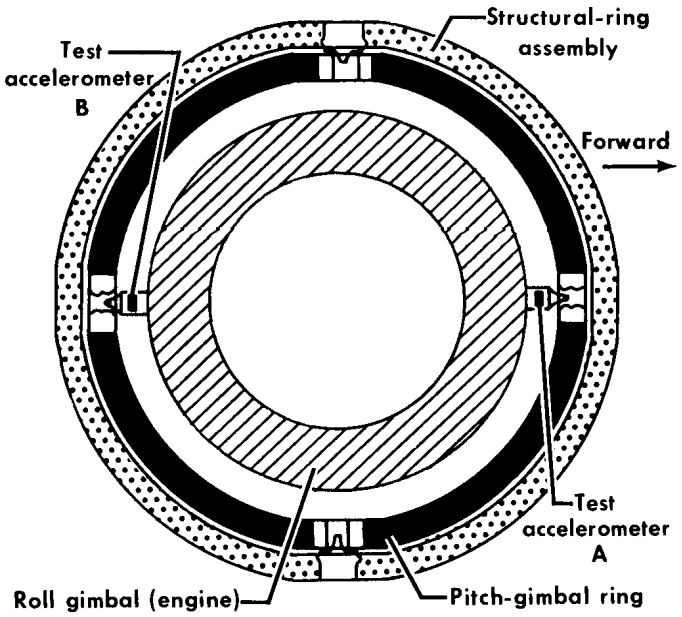

Figure 6.– Locations of accelerometers for jet stability tests.

pitch- and roll-gimbal-angle position and the outputs of accelerometers mounted on the roll trunnion mounts to sense vertical vibration. The locations of the accelerometers are shown in figure 6. The time history (fig. 5) is the response of the original jet-engine attitude system (engine-centered mode) with no input applied. A sustained pitch oscillation of constant amplitude is apparent with a frequency of approximately 7 cps. The outputs of the accelerometers mounted forward and aft on the roll trunnion mount are also in phase, which indicates that the primary motion of the pitch gimbal is in the vertical direction.

The dynamic-response characteristics of the gimbal structural assembly are presented in figure 7. These time histories were obtained from tests conducted by exciting the pitch, roll, and vertical structural modes of the gimbal system and recording the outputs of accelerometers that were placed on the vehicle to sense a particular mode. The structural vibrations were excited by suspending lead weights from wires attached to the structure and then cutting the wire,

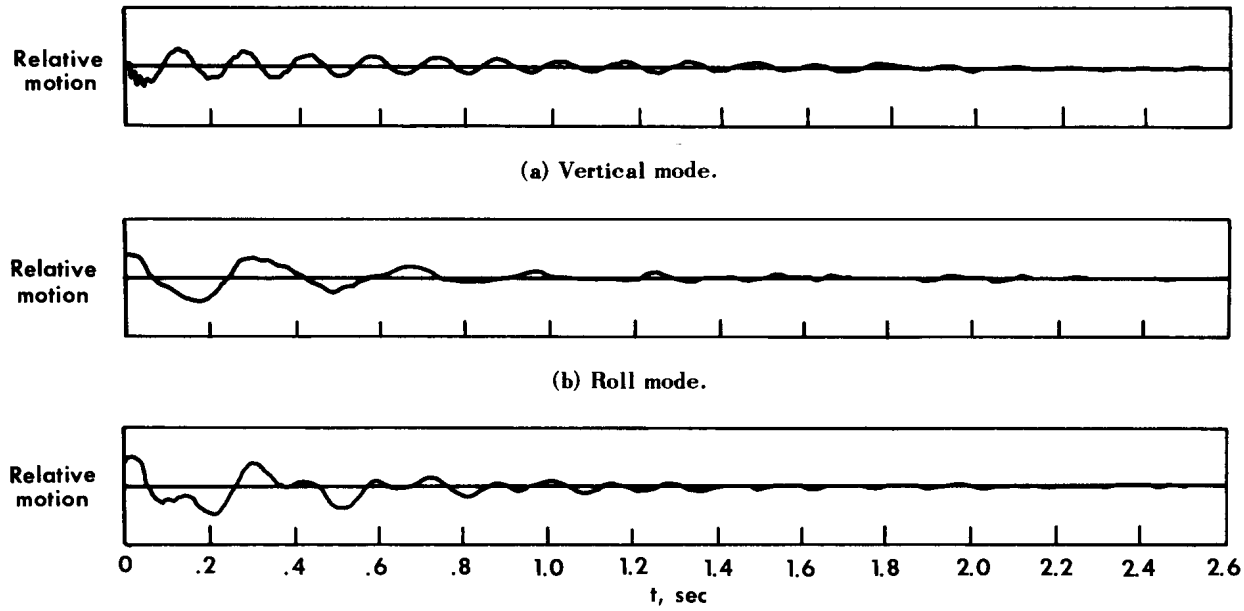

(a) Vertical mode.

(b) Roll mode.

(c) Pitch mode.

Figure 7.– Dynamic response of gimbal structural modes.

thus releasing the load on the structure. This technique resulted in an excellent localized impulse type of forcing function being imparted to the structure. Figure 7(a) shows the structural response to a vertically applied impulse, figure 7(b) the response to a roll impulse, and figure 7(c) the response to a pitch impulse. The natural frequency and damping of each mode as determined from the time histories are as follows:

Mode	ω_n, cps	ζ
Vertical	6.7	0.02
Roll	3.3	.1
Pitch	3.0	.1

Figure 7(c) shows that the vertical mode was also excited by the pitch impulse and appears as a 6.7-cps oscillation summed with the 3-cps pitch frequency. This 6.7-cps vertical vibration of the pitch gimbal was found to have a significant effect on the performance of the jet-engine attitude system and to be the cause of the instability shown in figure 5. The instability resulted from pitch-gimbal-angle sensors, used to provide a followup signal for the jet-engine attitude system, sensing the 6.7-cps frequency and attempting to drive the pitch gimbal at this frequency through the jet-engine attitude system. The input to the system from the pitch-gimbal-angle sensor further excited the vertical frequency, causing the oscillation to sustain itself with no external input.

In the original system configuration, the gimbal-angle sensors were fastened mechanically to the vehicle structure and coupled to the pitch and roll gimbals by a flexible linkage arrangement. This arrangement resulted in increased sensitivity of the sensors to the structural vibration, so the sensors were relocated such that actuator position was sensed rather than actual gimbal deflection. In this manner, the sensors were essentially isolated from the gimbal structural dynamics.

Attitude control system. – Structural vibrations were also of sufficient magnitude to excite the rate gyros used by the attitude control system as feedback sensors. This resulted in instabilities in the control system, which caused unstable operation of the attitude rockets.

The original location of the gyros on the aft platform of the vehicle is shown in figure 8. With the gyros in this location, three frequencies were found to be of sufficient magnitude to require attenuation in order to prevent excessive attitude-rocket

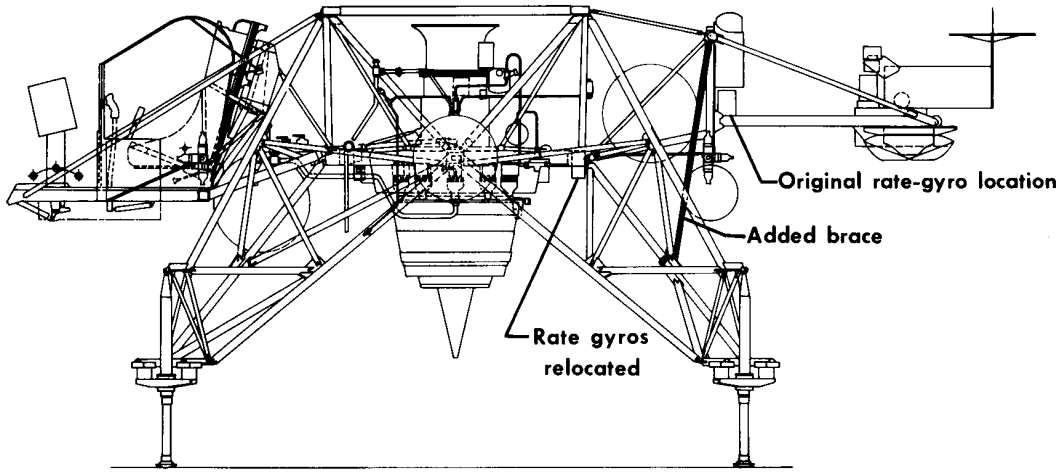

Figure 8.– Rate-gyro relocation.

operation. The frequencies were a 4-cps vertical vibration and an 8-cps torsional vibration of the aft-platform structure, on which the rate gyros were mounted, and a 20-cps resonance associated with the attitude-rocket cluster and vehicle structural-ring assemblies. The attenuation levels required at each of these frequencies to reduce the rate-gyro output signal so as not to exceed a 1 deg/sec (0.018 rad/sec) deadband setting are shown by the square symbols in figure 9. These levels were determined from tests conducted on the vehicle prior to any structural modification.

Although the 20-cps resonance associated with the attitude-rocket cluster and structural-ring assemblies was of sufficient frequency content to be filtered effectively without seriously deteriorating control response at lower frequencies, the 4-cps and 8-cps resonances were not. Since stiffening the platform assembly would have required the addition of considerable weight in order to completely eliminate the resonance problem, a compromise was made by (a) adding lightweight braces at the aft platform and rocket-cluster assemblies, (b) relocating the rate-gyro assembly to a more rigid mount less subject to the 4-cps low-frequency structural vibrations, and

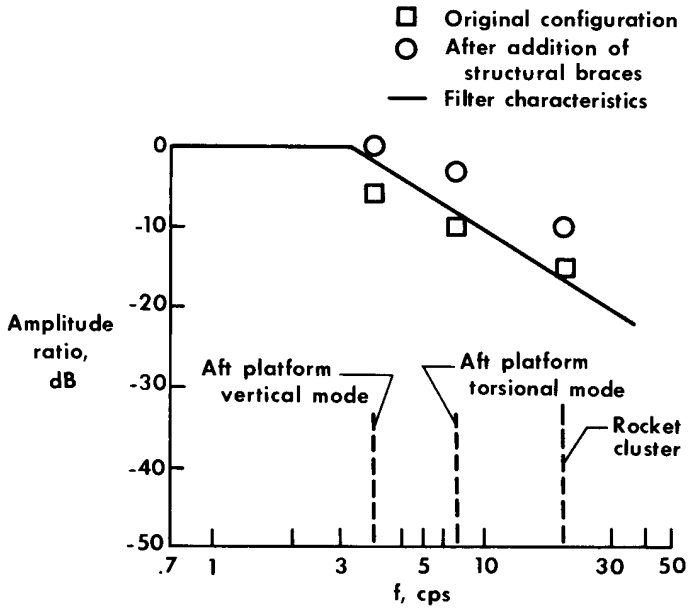

Figure 9.– Effect of electronic filtering and structural modifications in eliminating LLRV attitude control system response to structural modes.

(c) incorporating a filtering network to further attenuate the higher frequency signal levels.

The attenuation levels required at the structural frequencies after the braces were added and the rate gyros relocated are shown by the circle symbols in figure 9. The 4-cps aft-platform vertical-resonance problem was entirely eliminated by mounting the rate gyros to the vehicle structural ring at the junction of the rear-leg assemblies (fig. 8). The addition of the structural braces also considerably reduced the attenuation required at the 8-cps and 20-cps frequencies. A first-order filter with a corner frequency of 3 cps (solid line, fig. 9) was added to the system. This addition resulted in a 6-dB attenuation margin at the 8-cps and 20-cps frequencies that has proved to be effective in eliminating any ACS response to the structural frequencies.

Lunar-simulation system. – Closed-loop tests were conducted on the LLRV lunar-simulation system to assess the effects of the various structural frequencies on the system's response. The linear-acceleration feedback signals were computed from jet-engine attitude and throttle position, since dynamic ground tests were impractical. The following equations were employed by using small-angle approximations:

$$\ddot{z} = \frac{T_j}{m} + \frac{T_{lr}}{m}$$

$$\ddot{x} = \frac{T_j}{m}\Theta_g$$

$$\ddot{y} = \frac{T_j}{m}\varphi_g$$

A signal proportional to $\frac{T_j}{m}$ was obtained from a synchrotransmitter connected to the jet-engine throttle. The $\frac{T_{lr}}{m}$ signal was obtained from the thrust-to-weight computer, and the Θ_g and φ_g gimbal angles were obtained from potentiometer sensors. A simplified block diagram of the ground test setup for the pitch axis is shown in figure 10. The accelerometers were left connected to the system so that the response to any structural vibration would be experienced.

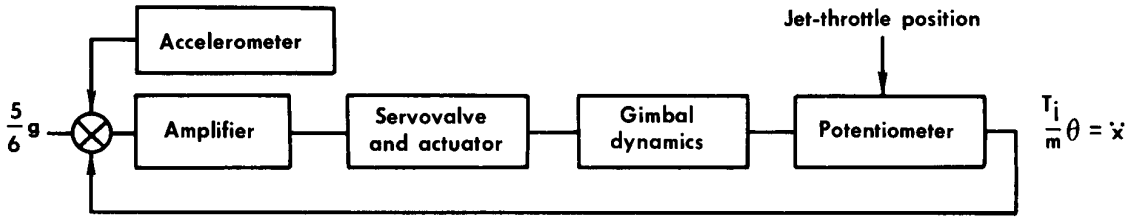

Figure 10.– Simplified block diagram of ground test setup for the pitch-axis jet-engine stabilization system closed-loop evaluation (similar diagram for roll axis).

In figure 11 the response of the original jet-engine stabilization system to a $\frac{5}{6}$ g input command is illustrated. The figure presents a time history of the pitch- and roll-gimbal position and the $\ddot{x}$- and $\ddot{y}$-accelerometer outputs. A sustained oscillation

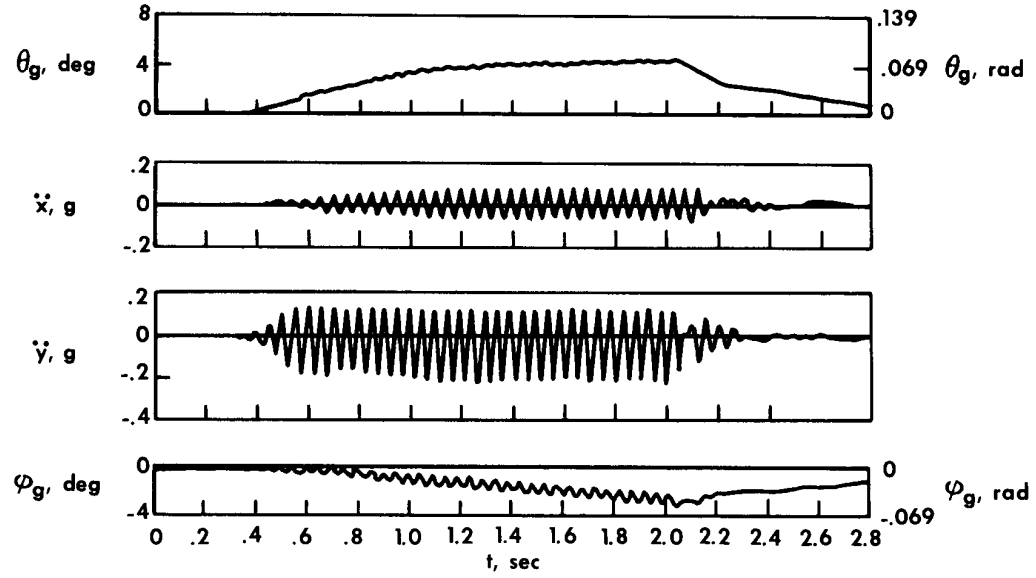

Figure 11.– Response of jet-engine stabilization system showing instability from structural vibration.

was experienced at the 20-cps resonant frequency of the structural-ring assembly. The resonance was sensed by the accelerometers and fed into the system driving the engine gimbals at this frequency, which further excited the oscillation. Since the outputs of the accelerometers used by the system were modulated 400-cps signals, the situation could not be corrected simply by filtering the output. It was necessary to modify the compensation network incorporated in the system for stabilization.

A block diagram showing the original compensation-network characteristics is presented in figure 12. The network consisted of two lead terms, at 0.48 cps (3 rad/sec) and 1.91 cps (12 rad/sec), a lag term at 6.84 cps (43 rad/sec), and an integrator. The transfer function for the servovalve and actuator was calculated. The computed

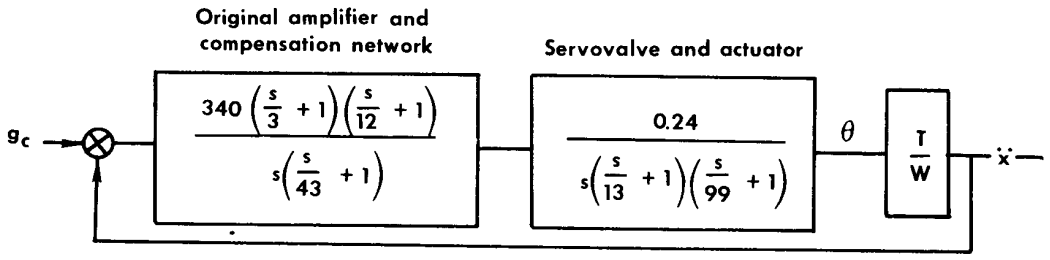

Figure 12.– Block diagram of original lunar-gravity simulation system (typical for pitch and roll).

open-loop frequency response of the original jet-engine stabilization system for one axis is shown in figure 13. The original system-crossover point occurred at a frequency of 4.4 cps (27.5 rad/sec) with a phase margin of 85° (1.5 rad).

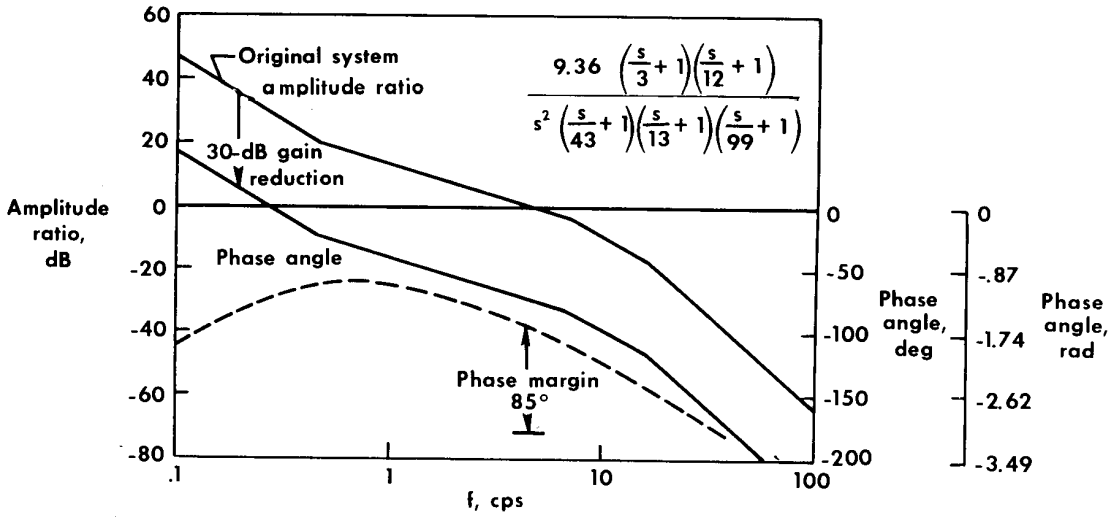

Figure 13.– Open-loop frequency response of the original jet-engine stabilization system.

Tests conducted on the vehicle indicated that a gain reduction of approximately 30 dB at the 20-cps point was required to prevent the system from responding to the structural resonance. From figure 13, it can be seen that a gain reduction of 30 dB would result in a gain crossover of 0.26 cps, which would sharply reduce the closed-loop bandwidth of the system. The compensation circuitry was subsequently modified to obtain a network that exhibited the desired attenuation at the higher frequency end (20 cps) but still possessed sufficient gain at low frequencies so that an adequate closed-loop bandwidth could be obtained.

In figure 14 an open-loop frequency response of the system with a network exhibiting the desired characteristics is presented. The attenuation level at the 20-cps frequency has been decreased by approximately 46.5 dB. The gain-crossover

frequency is 0.86 cps (5.4 rad/sec) and the phase margin is 40° (0.70 rad). The reduction in phase margin compared to the original network is attributed to the additional lags that were necessary to increase the attenuation at the higher frequencies.

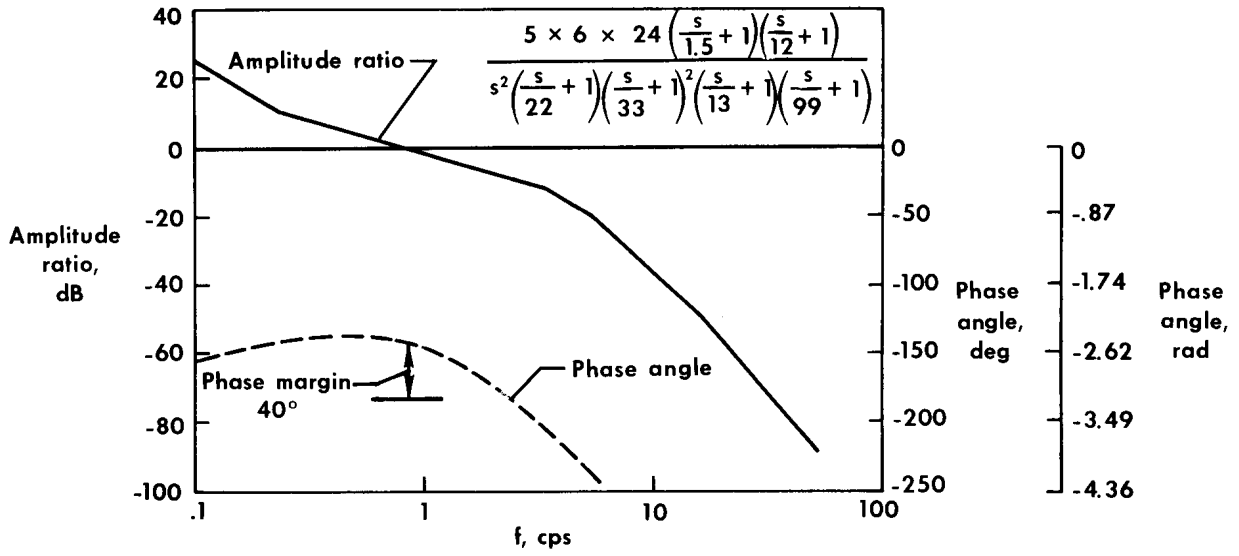

Figure 14.– Computed open-loop response of modified lunar-simulation system.

In figures 15(a) and (b) the original and modified closed-loop response characteristics of the jet-engine stabilization system are compared. The original system bandwidth was approximately 3 cps (point at which closed-loop response is down -3 dB).

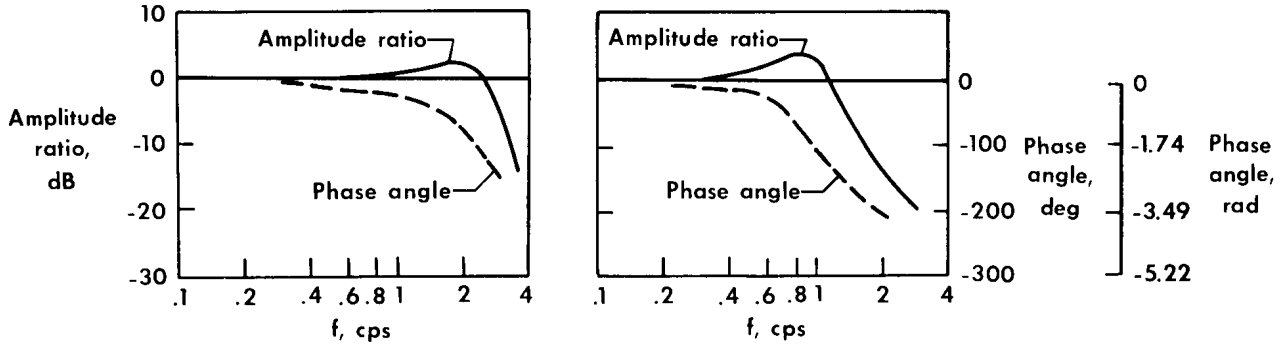

(a) Original shaping. (b) Modified shaping.

Figure 15.– Closed-loop frequency response of original and modified jet-stabilization systems.

The modified system, however, has a reduced bandwidth of approximately 1.0 cps brought about by the gain reduction necessary to eliminate the response of the system to the 20-cps structural resonance. A significant increase in the closed-loop peaking associated with the modified system is also apparent, which indicates a reduction in damping. The closed-loop response of the original and modified jet-engine

stabilization system to a step input is shown in figure 16. In figure 16(a) the response of the original system shows a 2° (0.035 rad) overshoot with a rise time of 0.4 second. In figure 16(b) the overshoot and rise-time overshoot of the modified system are approximately 3° (0.052 rad) and 0.4 second, respectively.

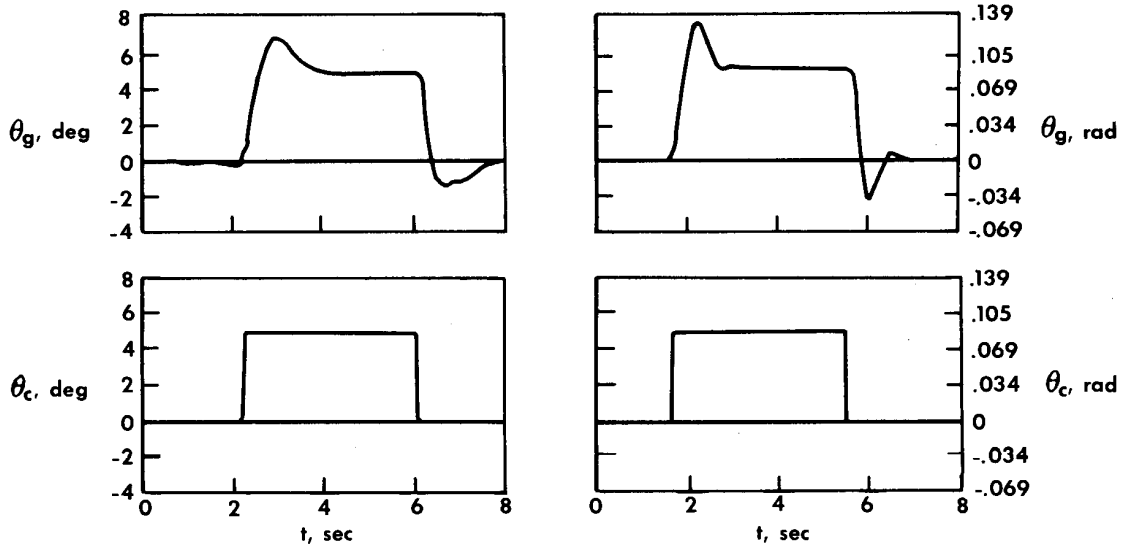

(a) Original shaping. (b) Modified shaping.

Figure 16.– Response of jet-stabilization system to step inputs.

Signal Modulation

Input signals to the LLRV flight control systems are modulated with a standard 400-cps carrier. Input networks are required to correct for phasing discrepancies between the various sensors because of the many signal summations that are necessary. The critical value of these networks and the accuracy required resulted in a significant amount of time-consuming experimentation to arrive at satisfactory component values. The effect of input-network accuracy on JSS and ATS operation is reflected in the closed-loop accuracy of these systems and small inconsistencies in phase compensation between the input and feedback signals being summed. In the vehicle attitude control system small errors in phasing can result in insufficient nulling for large inputs, which causes false failure indications and resultant transfer to the backup ACS.

LLRV Ground Tests

Before the LLRV flight-test program was started, a special ground test fixture was used to assess the effect of the various modifications to the flight control systems on the closed-loop-response characteristics of the systems. A photograph of the fixture with the LLRV attached is shown in figure 17. The fixture was designed to allow angular motion about the pitch or roll axes, one axis at a time. In the setup shown, rotation about the roll axis is possible, with rotation about the pitch axis being

fixed. The fixture attaches to the vehicle gimbal trunnions, allowing gimbal rotation independent of vehicle motion. In this manner, the jet-engine attitude control systems can be operated simultaneously with the attitude control system.

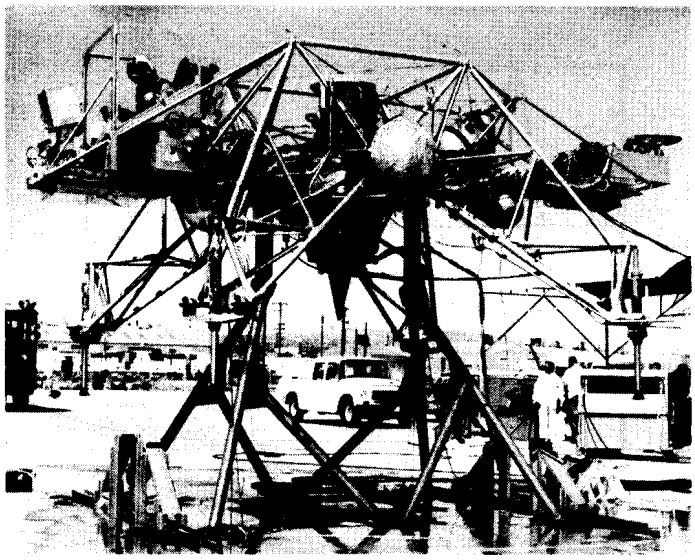

E-11939

Figure 17.– LLRV attached to ground test fixture.

Tests were conducted by having pilots fly single-axis control tasks with the JSS in different modes of operation. Tests were made both with the jet engine shut down and with the engine operating to determine the effect of engine noise, vibration, and temperatures on system response.

A second fixture was also used for ground tests and evaluation of the LLRV attitude control system. This fixture attaches to the lower portion of the jet engine and holds the engine fixed while allowing vehicle rotation about the pitch and roll axes through the gimbal arrangement. This fixture requires that the JSS hydraulic actuators be disconnected to allow freedom of rotation.

FLIGHT EXPERIENCE

The objectives of the first 34 flights of the LLRV were to develop the various systems to an operational level and to familiarize the pilot with the particular tasks associated with the vehicle. Flights 1 to 8 were for attitude control system evaluation; 9 to 11, pilot familiarization and maintenance checkout; 12 to 16, automatic-throttle system evaluation; and 17 to 34, jet stabilization system evaluation. For these flights, it was necessary to establish a set of ACS control parameters that would result in a vehicle response that would facilitate the pilot's evaluation of the jet-engine attitude and lunar-simulation systems. The results of a six-degree-of-freedom analog-simulator program were relied upon for the initial attitude-rocket thrust, threshold settings, and control sensitivities. The extensive ground test phase prior to the flight test program was instrumental in reducing the number of flights required to qualify all LLRV systems as operational. All of the systems discussed in the previous sections and in the appendixes have been tested during flight and found to perform satisfactorily. The flight experience with each system is discussed in detail in the following sections.

Attitude Control System

Table I summarizes the ACS control parameters investigated during the first 20 flights and the objectives of each flight. Since emphasis was placed on establishing

a satisfactory system to facilitate evaluation of the various other LLRV systems, no attempt was made to investigate controllability boundaries or minimum control requirements during these flights.

Limit cycle. – The first LLRV flight consisted of three different lift-offs, each made with the jet-engine attitude system in the local-vertical mode. The total airborne time was approximately 1 minute. Although the flight was to be made with only one set of attitude control rockets, a relay failure caused both sets to operate simultaneously, which resulted in twice the planned control effectiveness in each axis. The unexpected increase in control effectiveness produced limit-cycle oscillations about the vehicle pitch and roll axes. Although the limit-cycle oscillations were not objectionable from the control and stability standpoint, the resultant fuel consumption made the operation undesirable. The pilot rated the control task about the pitch and roll axes during the flight as 4 and 4, respectively, based on the Cooper scale (ref. 5).

Control-stick dead zone. – Although the LLRV attitude control system contains an inherent electrical dead zone associated with the control stick and rudder pedals, it became readily apparent during the first flight that the maximum dead zone attainable electrically with the center stick was not sufficient to prevent inadvertent pilot inputs. The dead-band characteristics of the center stick are illustrated in figure 18, which also shows several values of stick sensitivity investigated.

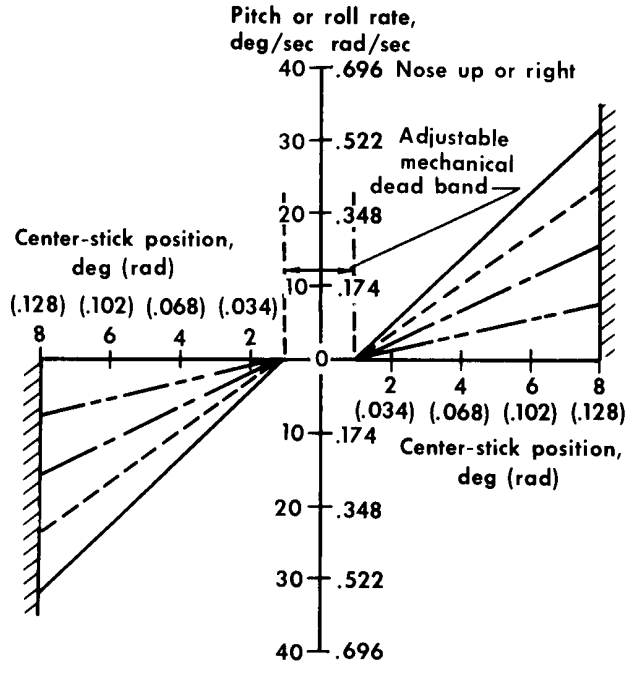

Figure 18.– LLRV angular rate command as a function of stick position.

The control parameters used for the first flight resulted in a center-stick dead zone of ±0.25° (±0.004 rad) for both pitch and roll and a yaw-pedal dead zone of 1.5° (0.026 rad). Since the maximum center-stick deflection in pitch and roll is 8° (0.14 rad), the stick dead zone was approximately 3 percent of the maximum stick travel. The yaw-pedal dead zone was approximately 6 percent of the maximum pedal travel (maximum = 25° (0.436 rad)). The pilot stated that, although he experienced little difficulty about the yaw axis, it was practically impossible to prevent inadvertent inputs with the center stick.

A mechanical dead zone was subsequently added to the center-stick synchros which, in effect, increased the 0.25° (0.004 rad) dead zone by an additional 1° (0.017 rad). This increased the overall center-stick dead zone to 15 percent of maximum deflection in both pitch and roll. Subsequent flights have shown this increment to be satisfactory in reducing inadvertent inputs with the center stick.

Yawing moment due to jet-engine exhaust. – During the early LLRV checkout flights, the presence of an external left yawing moment acting on the vehicle was detected. The disturbing moment was produced by the swirling motion of the jet exhaust, which imparted a force on the vehicle about the yaw axis. The moment varied with jet-engine rpm and for typical flights was on the order of 80 ft-lb (109 N-m). Figure 19(a) shows the duty cycle of the yaw attitude rockets, with the attitude control system operating in the rate command mode, in compensating for the disturbing torque. The yawing motion was not seriously detrimental to the controllability of the vehicle, although the hydrogen-peroxide consumption of the yaw rockets in compensating for the jet-engine exhaust swirl was undesirable. A jet-engine bleed-air nozzle was subsequently installed on the vehicle to counteract the yaw-left moment. The nozzle was located to generate a yaw-right moment of 80 ft-lb (109 N-m). By using jet-engine bleed air, the thrust of the counteracting nozzle also varies with jet-engine rpm in the same manner as the exhaust swirl.

Figure 19(b) is a time history of a later LLRV flight in which the anti-swirl nozzle was installed. A considerable reduction in rocket-on time and resultant fuel consumption is apparent.

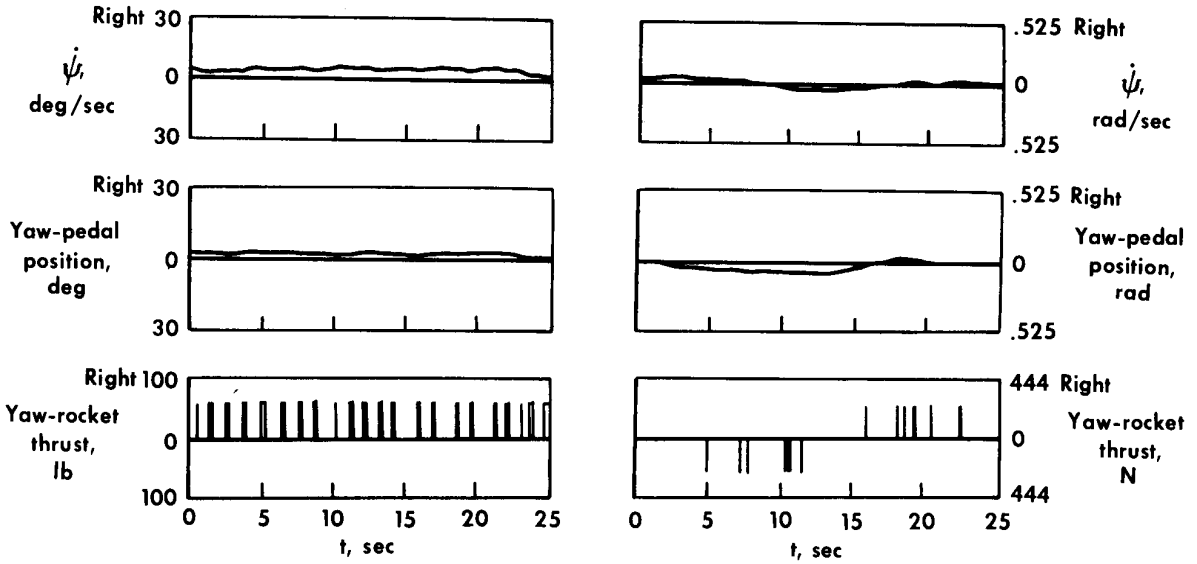

(a) No anti-swirl nozzle. (b) Anti-swirl nozzle used.

Figure 19.– Effect of jet fluid-air anti-swirl nozzle on yawing-moment compensation.

Open-loop control about yaw axis. – The operation of the LLRV rate command system in canceling vehicle motions resulting from external disturbances is illustrated in the time history of figure 20. During the early portion of the time history, the yaw-right rockets were pulsing continuously in an attempt to cancel the yaw-left disturbing moment resulting from the jet-exhaust swirl. The yaw rate of the vehicle was reduced to the 2 deg/sec (0.035 rad/sec) yaw-rate dead band. At the point in the time history indicated by the dashed line, the yaw primary controls failed and the system automatically transferred to the backup mode of control, which is on-off acceleration command. The pilot had to manually correct for the external yawing moment, which

is indicated by the increase in yaw-pedal inputs. It is interesting to note the difference in the control technique experienced with the rate and acceleration command systems. The higher pulse rate of the rate command system results in tighter control with very few pilot inputs and in a rate of fuel consumption of 10 lb/min (44.5 N/min). The acceleration command system results in coarser control with much more pilot attention required but a reduced rate of fuel consumption of 7.4 lb/min (32.9 N/min).

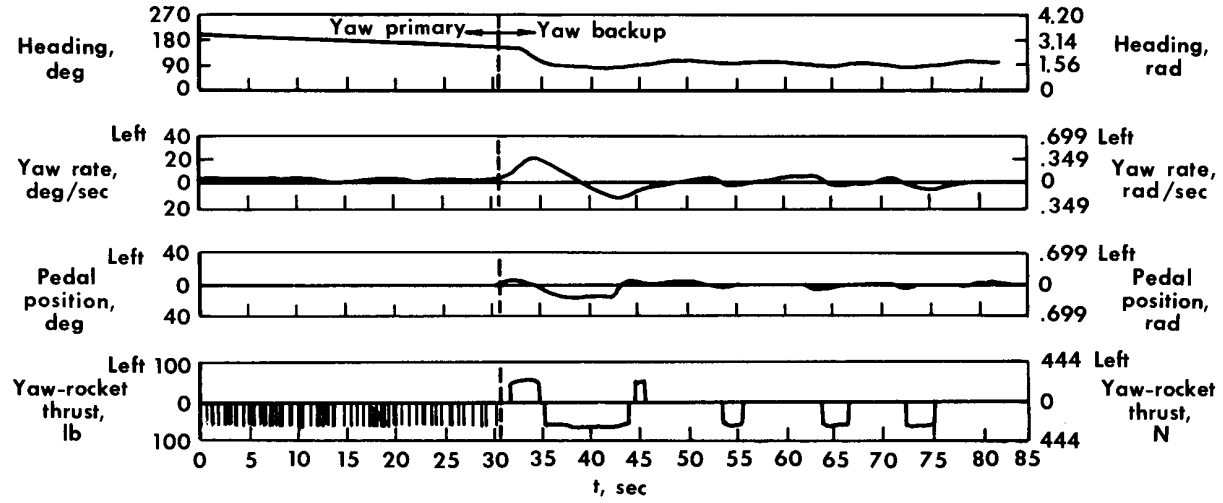

Figure 20.– Time history showing a yaw-damper failure.

Jet-Engine Attitude Control Systems

Prior to the LLRV flight test program, a six-degree-of-freedom fixed-base simulator investigation was conducted at the NASA Flight Research Center to evaluate LLRV control requirements. The results of this investigation indicated that the control task associated with the vehicle while operating in the jet-engine local-vertical mode was considerably easier than when operating in the gimbal-locked or engine-centered modes. The simulator studies showed that translational velocities of the vehicle in the gimbal-locked mode were extremely sensitive to small changes in vehicle attitude angles, since the relatively large thrust of the jet engine was being vectored. When operating in the local-vertical mode, however, the jet engine remains vertical, regardless of vehicle attitude, and translational velocities are the result of vectoring the much smaller lift-rocket thrust. The vehicle attitude control task was therefore significantly reduced, because small vehicle attitude changes have slight effect on vehicle translation. The visual presentation of translation presented to the pilot on the simulator was a small x-y plotter.

As a result of these simulator studies, it was decided to make the first test flights with the LLRV jet-engine attitude system in the local-vertical mode. In actual flight, however, the marked contrast between the control tasks associated with gimbal-locked and local-vertical modes derived from the analog-simulator studies did not materialize. In fact, pilots indicated a preference for the gimbal-locked (VTOL) mode

of operation over the local-vertical mode, indicating that a more positive control of vehicle translation was possible in the gimbal-locked mode. This preference is attributed primarily to motion and environmental cues of the real world (i.e., free-flight craft) which were not present during the analog studies. The pilots found the use of visual and motion cues to be valuable in accomplishing translation maneuvers by vectoring the large jet-engine thrust in the gimbal-locked mode. In addition, the pilots stated that the relatively large angles and time required for translation in the local-vertical mode were "new" and required additional learning and adjustment.

Lunar-Simulation System

After the operational status of the vehicle and jet-engine attitude control systems was demonstrated satisfactorily, flight testing of the lunar-simulation system was undertaken. Since it was possible to operate the automatic-throttle system independently of the jet-stabilization system, the program was accomplished in two phases: (1) checkout of the automatic-throttle system and (2) checkout of the jet-stabilization system.

Automatic-throttle system. – Figure 21 is a time history showing the operation of the LLRV automatic throttle during a landing maneuver in which the jet-stabilization system was not used for aerodynamic-drag compensation. Operation of the lift-rocket throttle was initiated at $t = 0$ second at an altitude of approximately 135 feet (41.2 meters). The automatic-throttle mode was automatically engaged by the initial weighing circuitry at $t = 1$ second. This corresponded to a total upward acceleration change of 0.104g, which resulted from the lift-rocket operation during the period from $t = 0$ second to $t = 1$ second. Since the system was preset to engage automatically when the upward acceleration resulting from lift-rocket operation reached 0.1g, an error of approximately 4 percent in the actual weight of the vehicle was realized. The pilot then reduced the lift-rocket thrust in order to arrest his upward acceleration and establish a hover. The jet-engine thrust decreased automatically and stabilized at a level equivalent to approximately 0.82g.

The computed normal-acceleration signal is also presented in figure 21 in order to better assess the accuracy of the system. The overall accuracy experienced with the automatic-throttle system between the commanded vertical acceleration and the actual vertical acceleration obtained has been on the order of ±0.02 earth g. The two major sources of error in the system are the initial weighing circuitry and the reduced bandwidth required to filter the accelerometer noise components. This accuracy could be improved by minor modifications to the initial weighing circuitry and by increasing the automatic-throttle closed-loop bandwidth. The ±0.02g accuracy is not detrimental to the research goals set for the vehicle, however, and no program for improving this accuracy has been undertaken.

In the time history of figure 21, the pilot began his descent to touchdown at $t \approx 56$ seconds. Touchdown occurred at $t \approx 100$ seconds, at which point the jet-engine local-vertical mode was automatically selected by microswitches on the leg struts. The pilot stated that the landing maneuver was smooth and relatively easy to accomplish in comparison with landings in which the jet throttle was used for primary thrust control. Although the difference in the dynamic-response characteristics of the two thrust systems is appreciable, the reduced thrust gradient associated with

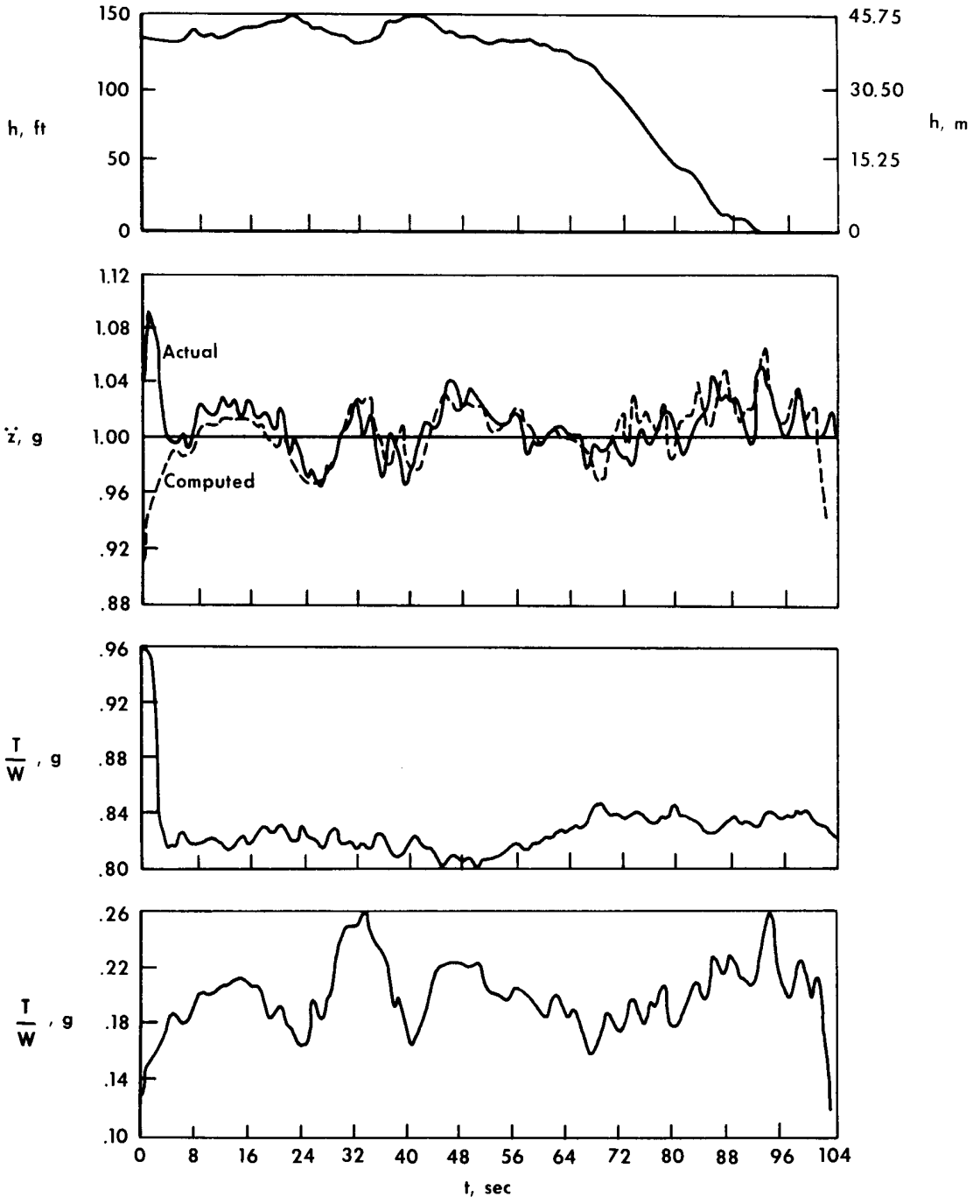

Figure 21.– Flight time history of LLRV automatic-throttle operation.

the lift-rocket throttle was judged by the pilots to be the reason for improved touchdown control.

Jet-engine stabilization system. – Because of the mechanization technique of the lunar-simulation system, it is not possible to operate the LLRV jet-stabilization system independently of the automatic-throttle system. It is necessary to engage the automatic-throttle system prior to transfer into the jet-stabilization system and full lunar-simulation operation.

A time history showing the operation of the lunar-simulation system during an LLRV landing maneuver is presented in figure 22.

Operation of the lift-rocket throttle was started at $t = 0$ second, and the initial weighing action was completed at $t = 1.5$ seconds, at which point the automatic-throttle system was automatically engaged. The pilot then arrested the vertical acceleration by reducing lift-rocket thrust, and the jet-engine gimbal-locked mode was disengaged at $t = 8$ seconds, which placed the vehicle in the full lunar-simulation mode. The pilot stated that no noticeable transient occurred when the gimbals were unlocked, even though the vehicle was at 2° (0.035 rad) left-bank angle.

For attitude angles less than 10° (0.17 rad), the $\ddot{x}$ and $\ddot{y}$ vehicle accelerations were accurate to within 0.01 earth g of the command values. For vehicle pitch attitudes greater than 10° (0.17 rad), the $\ddot{x}$ error was increased to approximately 0.02 earth g, which is indicative of a small $\ddot{x}$ gain error. This value is considered to be within the desired acceleration-error limits of the system.

At $t \approx 10$ seconds (fig. 22), the pilot initiated a nose-down pitch attitude to establish a forward translational velocity of about 10 ft/sec (3.05 m/sec). He then pitched the vehicle to a nose-up attitude (approximately 17° (0.29 rad) maximum) until the forward velocity was arrested and a rearward velocity was established. The vehicle was then pitched forward, the rearward translation stopped, and a simultaneous descent was initiated at $t = 50$ seconds from the translation altitude (approximately 90 ft (27.4 m)) to a landing hover. Touchdown occurred at $t = 78$ seconds. During the landing, the rear legs contacted the ground before the front legs. This was not intentional by the pilot but resulted from last-minute hover corrections to stop ground drift and from the desire to touch down within a reasonable time because of fuel limitations.

During the transition from a 17° (0.29 rad) pitch-up attitude to a 17° (0.29 rad) pitch-down attitude in the interval from 39 seconds to 53 seconds (fig. 22), the vehicle pitch attitude and the pitch-gimbal angle differ by approximately 4° (0.07 rad). This difference is a result of the jet engine being tilted from the vertical position to compensate for longitudinal drag forces acting on the vehicle during translation. During the pitch-down maneuver, which occurs while the vehicle is translating in a rearward direction, an increase in drag, resulting from more area being exposed to the velocity vector, tends to decrease the translational acceleration more rapidly than would be experienced in a near-vacuum environment such as would be encountered on the lunar surface. The attitude of the jet engine is then tilted to oppose the decrease in acceleration resulting from aerodynamic drag.

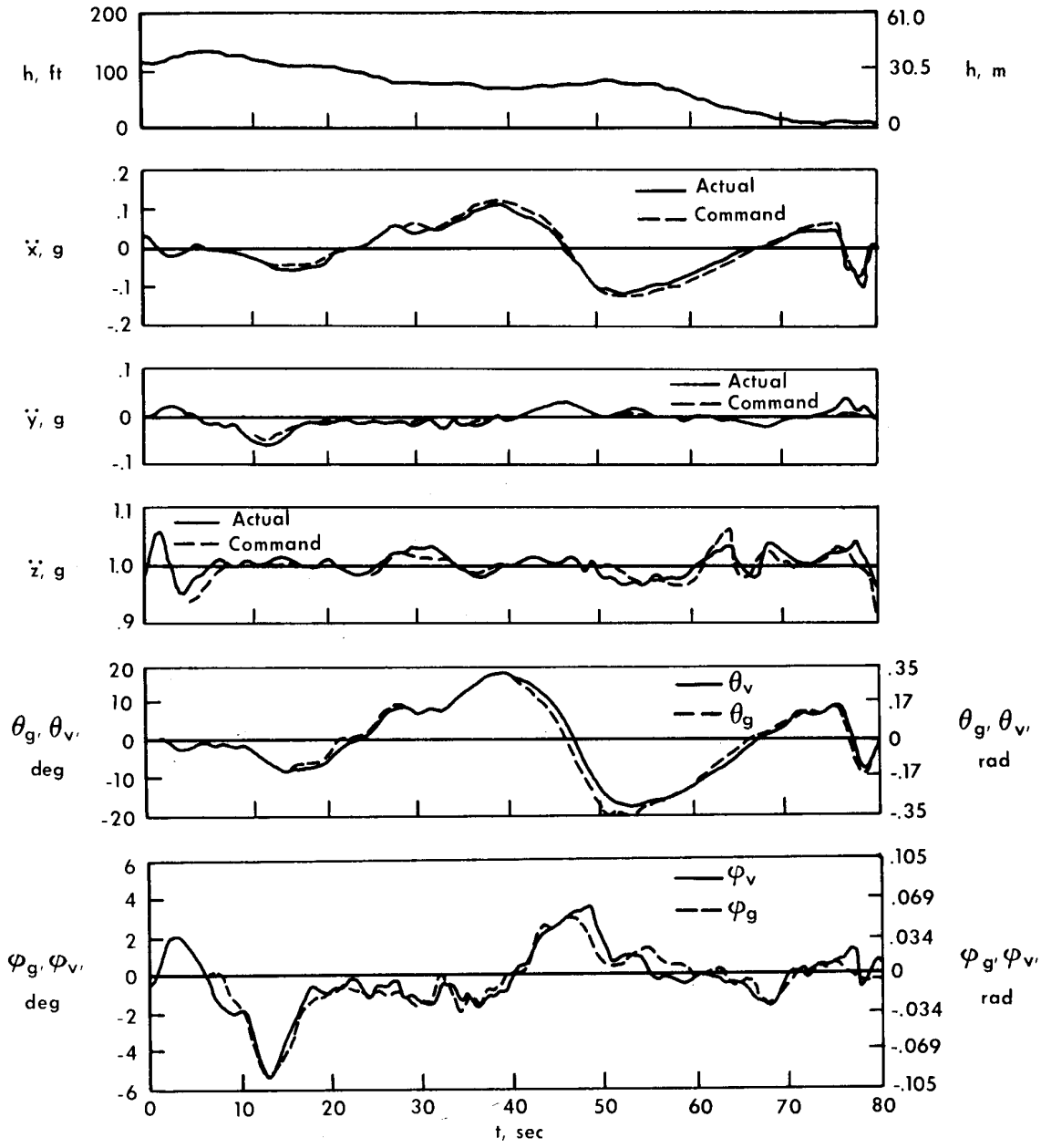

Figure 22.– Flight time history of LLRV lunar-simulation-system operation during a landing maneuver.

The pilots tend to rate the control task during the lunar simulation similarly to that experienced in the local-vertical mode of operation. The pilots describe the feeling of flying in the lunar mode as one of "slow motion" compared to VTOL operation. Large attitude angles are required for translation maneuvers which must be held for a significant period of time to generate desired translational velocities. The pilot is also forced to lead the translational motions and to apply corrective attitude inputs early in order to decrease velocities over a prescribed marker. He is thus forced to operate at much larger attitudes and for longer durations than required for conventional VTOL operation. This type of translation control (i.e., lunar-gravitational response) requires the pilot to use a greater degree of anticipation than normally needed in earth VTOL (LLRV gimbal-locked) operation. A natural result was for the pilots to use small vehicle angles and to keep the vehicle translation rate low until some learning and confidence were acquired. The pilots tended to overshoot in translation in the early lunar-simulation flights until a certain degree of learning was accomplished. Even after the pilots had been exposed to and operated in the lunar environment for several flights, they were still aware of the different flight environment and the techniques required to control precisely.

SYSTEM RELIABILITY

The advantages of weight, performance, and versatility of fly-by-wire systems as compared to mechanical and hydraulic systems are strong factors in favor of this type of control. The primary disadvantage of fly-by-wire controls, however, is reduced confidence in system reliability. In any fly-by-wire control system where a pilot must rely entirely on electronics to provide adequate vehicle stability and control, reliability of the various electronic hardware is of utmost concern. Reliability of the electronic circuitry and components of the LLRV flight control systems has, in general, been good. An in-flight failure history of the LLRV systems is presented in figure 23. The solid line shows the number of failures that occurred during actual flights of the vehicle. In table II a failure log is presented in which the types of malfunctions experienced during flights and ground tests are listed.

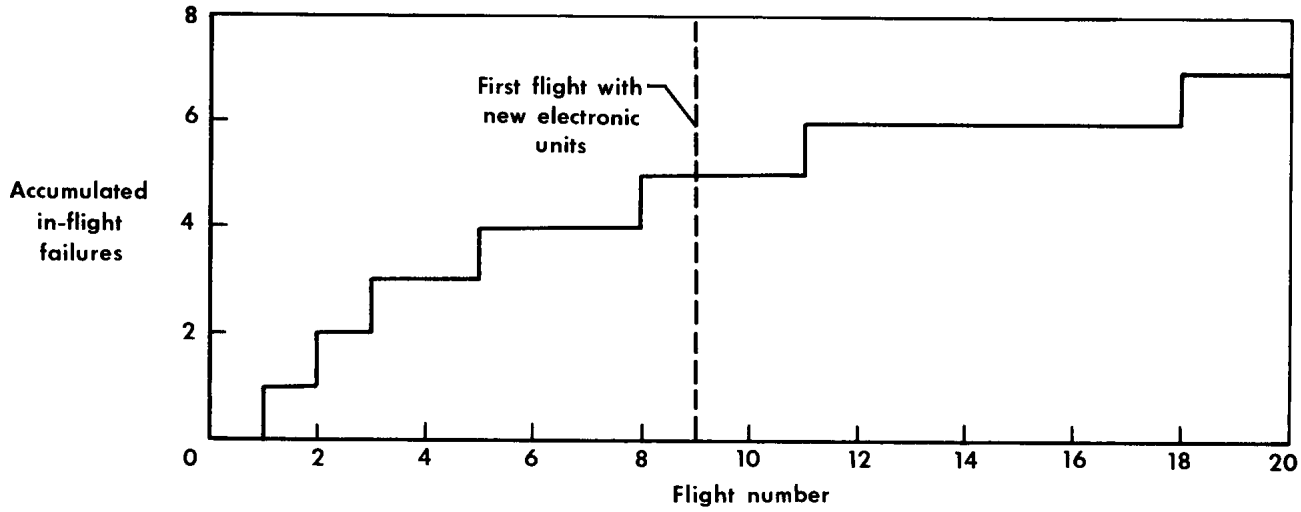

Figure 23.– In-flight failure history of LLRV electronics.

As might be expected, the highest frequency of in-flight failures occurred during the early LLRV flights. It is interesting to note, however, that most of the failures were the result of loose terminal connections and wire breakage, rather than actual component failure. Three major items were believed to have contributed significantly to this type of failure. These items are discussed in detail in the following sections.

Lightweight Chassis Construction

The original LLRV avionics chassis assemblies were constructed from lightweight aluminum, with considerable emphasis placed on weight-saving techniques. During vibration tests of the electronic units, the lightweight construction was found to result in low-frequency resonances which caused several system malfunctions. The weak structural areas were subsequently modified and stiffeners were added to provide more support. Large components, such as filter capacitors and relays, that were especially subject to resonant vibrations were firmly attached to the electronic assemblies by use of a potting compound to provide extra strength. The units were then subjected to additional vibration tests to insure satisfactory performance.

In view of this problem, a second set of electronic hardware, for flight operation, was constructed utilizing a heavier aluminum chassis material. These units readily passed the vibration tests and were installed in the vehicle after flight number 8. It is significant to note the reduction in failures associated with the heavier units as compared to the lightweight boxes.

Extensive Component Changes

Another possible contributing factor to the initial failure rate shown in figure 23 was the extensive circuitry modification phase that was brought about by the various problems encountered with the avionics. Since these problems did not become apparent until the final stages of closed-loop response tests on the vehicle, the electronic hardware had already passed qualification tests during which many components had been "potted" permanently to the chassis. During the modification to the various units, it was necessary to remove some of these permanently affixed components by manually chipping away the potting compound with varying degrees of physical force. Although this task was carried out with extreme care and was subsequently subjected to inspection, some structural weaknesses in the chassis assemblies could have resulted. This weakening would have also contributed to the higher failure rate before the second set of hardware (heavyweight chassis) was incorporated.

Construction of Printed Circuit Boards

The printed circuit-board assemblies used by the LLRV electronic circuitry utilize terminal junctions which rely on solder connections with extremely small wire for leads into and out of the various boards. Experience has shown that these leads are susceptible to breakage at the terminals during routine troubleshooting. The terminals have also shown a tendency to loosen and become subject to jet-engine

vibration, which results in a malfunction during flight although performance on the ground is satisfactory.

In view of the problems experienced with this type of printed-circuit connections, it is believed that a plug type of connector with a lock-tight mechanism would be more desirable from a reliability standpoint.

CONCLUDING REMARKS

The electronic flight control systems of the lunar-landing research vehicle (LLRV) have proved to be satisfactory in providing a free-flight test bed for investigation of pilot-controlled landings in a pseudolunar environment. The bang-bang, fly-by-wire rate command attitude control system has been effective and reliable in providing pilot control of vehicle attitude during all operations investigated. The wide range of parameter variations provides a versatile control system for research investigations. The jet-engine attitude control systems have shown satisfactory response characteristics and excellent reliability while providing control of jet-engine attitude during LLRV flights. The LLRV lunar-simulation system has been effective in automatically controlling jet-engine thrust and in providing a 1-lunar-g gravity vector acting on the vehicle and compensating for lift and drag aerodynamic disturbances. A lunar-gravitational environment is effectively simulated by the electronic system and is accurate during hover and translation maneuvers to within 0.02 earth g.

Pilots have found operation in a lunar environment to require a markedly different control technique than that used in conventional vertical takeoff and landing (VTOL) operation. During lunar-simulation operations, the pilot is forced to lead the translational motions and to apply corrective attitude inputs early in order to decrease velocities over a prescribed marker. He is thus forced to operate at much larger attitudes for longer durations than required for conventional VTOL operation. This type of translation control (i.e., lunar-gravitational response) requires the pilot to use a greater degree of anticipation than normally required in earth VTOL (LLRV gimbal-locked) operation.

Pilots found the use of motion and visual cues to be valuable in accomplishing translation maneuvers by vectoring the large jet-engine thrust in the gimbal-locked mode. For this reason, pilots indicated a preference for the gimbal-locked (VTOL) mode of operation over the local-vertical mode, which indicates that a more positive control of vehicle translation was possible with the gimbals locked. This effect was not perceived during fixed-base simulator studies.

Flight Research Center,
National Aeronautics and Space Administration,
Edwards, Calif., July 5, 1966.
924-23-21-13-72

APPENDIX A

DETAILED DESCRIPTION OF THE LLRV ATTITUDE CONTROL SYSTEM

A simplified block diagram showing the basic operation of a single channel of the LLRV attitude control system (ACS) is presented in figure 24. A conventional center

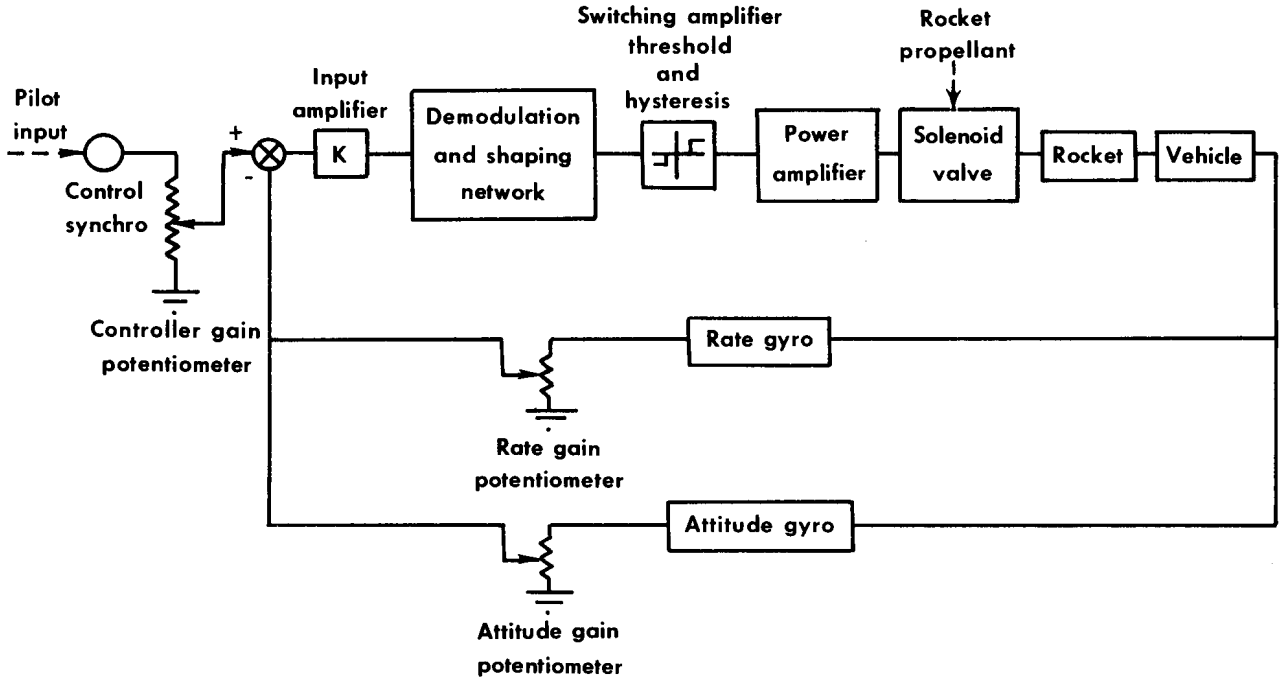

Figure 24.– Simplified block diagram of LLRV attitude control system (typical for all three axes).

stick is used for pitch and roll control, and rudder pedals are employed for yaw control. All sensing elements and control synchros are excited with 400-cycle ac electrical power. The control synchros are used to convert the controller motions (pilot inputs) to proportional electrical signals. These input signals are then summed with a feedback signal, resulting in an error proportional to either vehicle rate or attitude. The error signal is then fed to an input amplifier which is normally operated at unity gain (K = 1). A ground adjustment is provided so that the amplifier gain may be increased by a factor of 10 for higher open-loop gain and tighter dead-band operation. The output of the amplifier is then demodulated and applied to the input of a switching amplifier.

A circuit diagram of the switching amplifier and the associated circuitry is shown in figure 25. Three signals are summed at the input of the amplifier: the demodulated error signal, a threshold voltage which must be exceeded in order to fire the switching amplifier, and a hysteresis signal adjustment. The threshold voltage is determined by

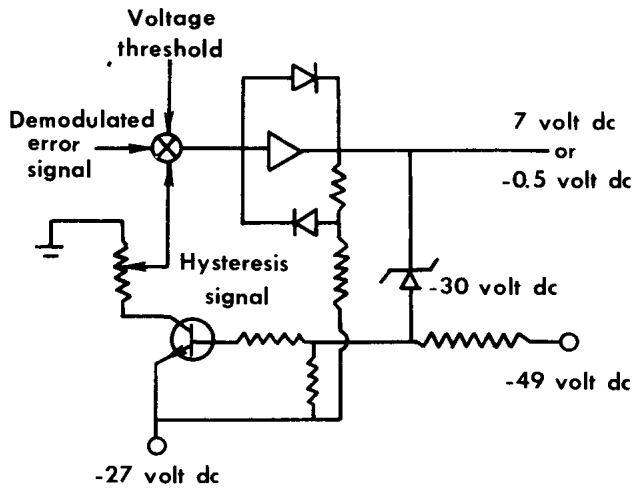

Figure 25.– Circuit diagram of switching amplifier.

a ground adjustable potentiometer and is set to correspond to a particular vehicle angular rate or attitude, depending on the mode of operation. The variable hysteresis signal is obtained from a separate solid-state switching circuit which lowers the voltage required to shut off the switching amplifier after the amplifier has been fired initially. This results, then, in a lower "off" threshold than "on" threshold. A diagram showing the effect of the threshold and hysteresis adjustments is presented in figure 26. The input voltage shown is the sum of the threshold, hysteresis, and demodulator error-signal summation and is used to fire the switching amplifier. The output of the amplifier is then fed to a power amplifier, which increases the signal strength to a sufficient magnitude to operate the on-off attitude-rocket solenoid propellant valves which control the flow of hydrogen-peroxide to the attitude rockets.

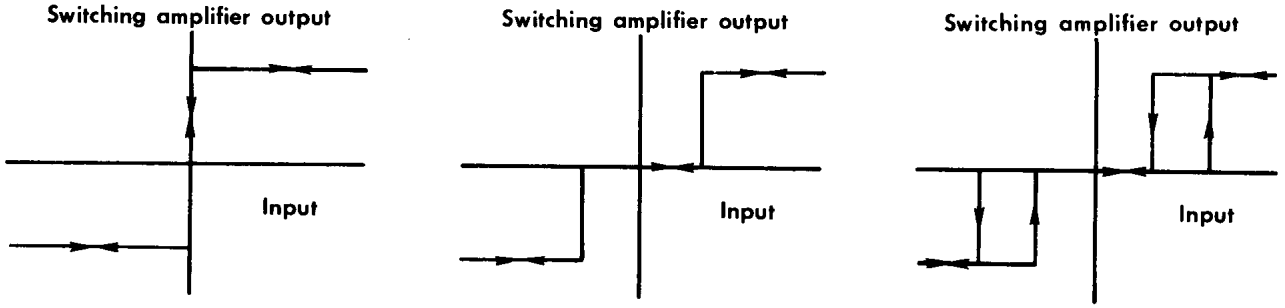

(a) Zero threshold and zero hysteresis.

(b) Threshold level with zero hysteresis.

(c) Threshold and hysteresis.

Figure 26.– Diagram showing the effect of threshold and hysteresis adjustments used in attitude control system.

Special provisions are also incorporated into the ACS circuitry to insure that the attitude rockets always respond in pairs to pure pitch, roll, or yaw inputs. The mechanization used to accomplish this simultaneous operation is shown in figure 27. For a pure pitch-command input the rocket-firing logic calls for an A and a B rocket, either standard or test, to fire simultaneously. However, because of inherent gain differences and practical limitations in the electronic circuitry, differences in signal levels invariably occur which result in one rocket firing before the other. Since this would result in both a pitch and a roll moment being applied to the vehicle, the operation is obviously not desirable. The situation is alleviated by decreasing the switching amplifier threshold of the opposite rocket when one rocket of a pair is fired. In figure 27, for example, if rocket A (standard or test) fires corresponding to a pure $+\Theta$ input, a negative-going voltage is applied to the threshold of the switching amplifier controlling

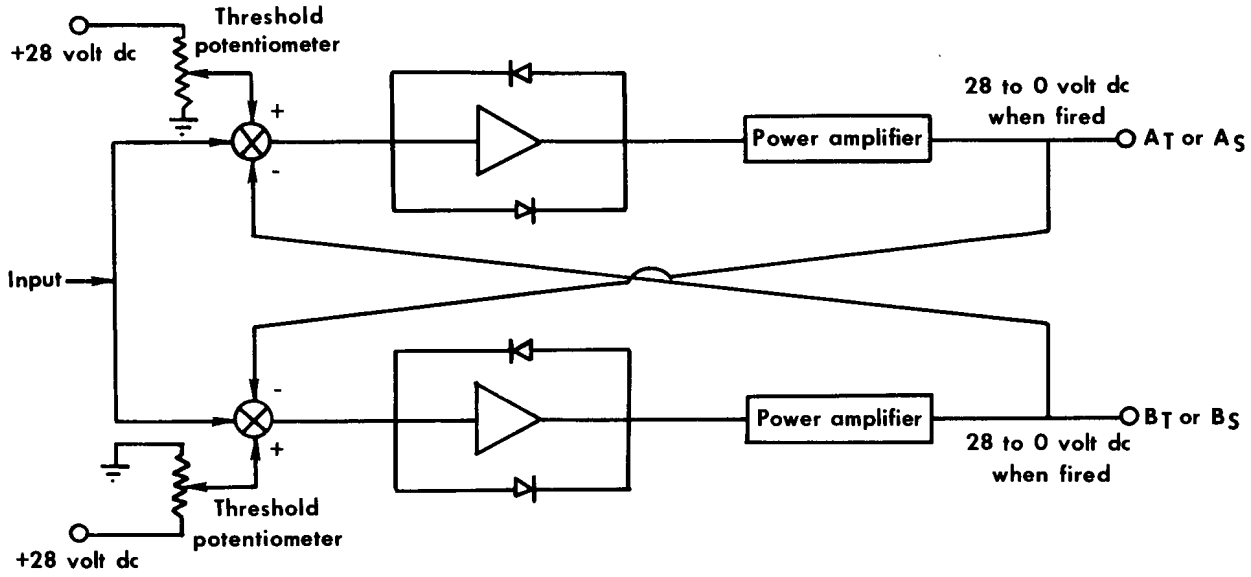

Figure 27.– Circuitry used to insure simultaneous operation of rocket pairs.

the operation of rocket B (standard or test). This results in a small decrease in the threshold voltage, which causes the switching amplifier and rocket B to fire. Since the rocket B switching amplifier is initially on the verge of firing, only a slight decrease in the threshold is necessary. Should rocket B fire first, the rocket A switching amplifier threshold is likewise decreased slightly. The maximum amounts of threshold reduction in terms of vehicle angular rate, attitude, and command input are as follows:

Rate $\approx$ 0.2 deg/sec (0.0035 rad/sec)

Attitude $\approx$ 0.25 deg (0.0042 rad)

Rate command $\approx$ 0.1 deg/sec (0.0015 rad/sec)

Attitude command $\approx$ 0.1 deg (0.0015 rad)

In normal operation at reduced gain settings, the threshold reduction is much less.

The mode of operation of the LLRV attitude control system is determined by the parameter that is fed back and compared with the pilot's input signal. The system is capable of providing both angular rate and attitude-feedback signals. The magnitude of these signals is also determined by individual potentiometer settings.

The acceleration command mode is selected by setting the rate and attitude gain potentiometers (fig. 24) to zero. The system is then operated in an open-loop manner by the pilot controlling the on-off thrust of the various attitude rockets. No feedback is used, and any damping moments must be provided by the pilot.

The rate command mode is selected by increasing the rate-feedback-gain potentiometer (fig. 24) while maintaining zero attitude feedback. The angular rate of the vehicle is then compared with the pilot's command input. If a discrepancy exists that exceeds the rate threshold, the attitude rockets are fired in a corrective manner.

The maximum commandable rates (40 deg/sec (0.61 rad/sec) about all three axes) for the LLRV attitude control system when operated in the rate-command mode are determined by the maximum output of the rate-gyro sensors.

The attitude-command mode is selected by incorporating an attitude-feedback signal in addition to rate feedback. This is accomplished by adjusting an attitude-feedback-gain potentiometer (fig. 24). Both the attitude- and rate-feedback signals are then compared with the pilot's command input. Should an error exist that is greater than the threshold setting, which is now proportional to both vehicle angular rate and attitude, the attitude rockets are fired. The maximum tilt angle of the vehicle is dictated primarily by the maximum gimbal-angle deflections, which are ±40°(±0.61 rad) in pitch and ±24° (±0.42 rad) in roll. No limit exists about the yaw axis.

Attitude Control System Monitor

The scheme used in the LLRV attitude control system to detect a malfunction in the electronic circuitry is illustrated in figure 28. The system consists of two separate channels designated as primary and monitor. In normal operation, the primary channel is used to control the operation of the attitude rocket. The monitor channel consists of electronic circuitry identical to that of the primary channel up to and including the switching amplifiers. At this point, a comparator circuit compares the outputs of the primary- and monitor-channel switching amplifiers. If a discrepancy exists, the comparator sends a signal to a relay which transfers the system from primary to backup electronics. The comparator output is delayed for approximately 0.15 second to reduce the susceptibility of the system to transients. The input and output signals of the primary power amplifiers are also compared. A discrepancy between these two points also results in a transfer to backup controls.

A failure in either the pitch or roll primary channels automatically transfers the system to both pitch and roll backup. A failure in the primary yaw circuitry transfers the system to yaw backup control only.

The pitch and roll backup ACS is a rate command system employing separate rate gyros from the primary system as feedback devices. Separate controlling synchros for backup control inputs are also used. The yaw backup ACS is an acceleration on command system, with the pilot operating the yaw attitude rockets directly by means of microswitches connected to the yaw pedals. No feedback is used in the yaw backup mode.

In order to compensate for slight gain differences between the primary and monitor circuitry, the initial threshold level of the monitor-channel switching amplifiers is set higher than the threshold level of the primary-channel switching amplifier. This insures that the primary amplifier is energized, and the threshold level of the corresponding monitor-channel amplifier is reduced to a level slightly below that of the primary channel. If the particular monitor amplifier involved is close to firing, this decrease in threshold level will turn it on. This eliminates the possibility of either a primary or a monitor amplifier being on separately unless an actual malfunction has occurred. The technique is similar to that used to insure simultaneous operation of attitude-rocket pairs.

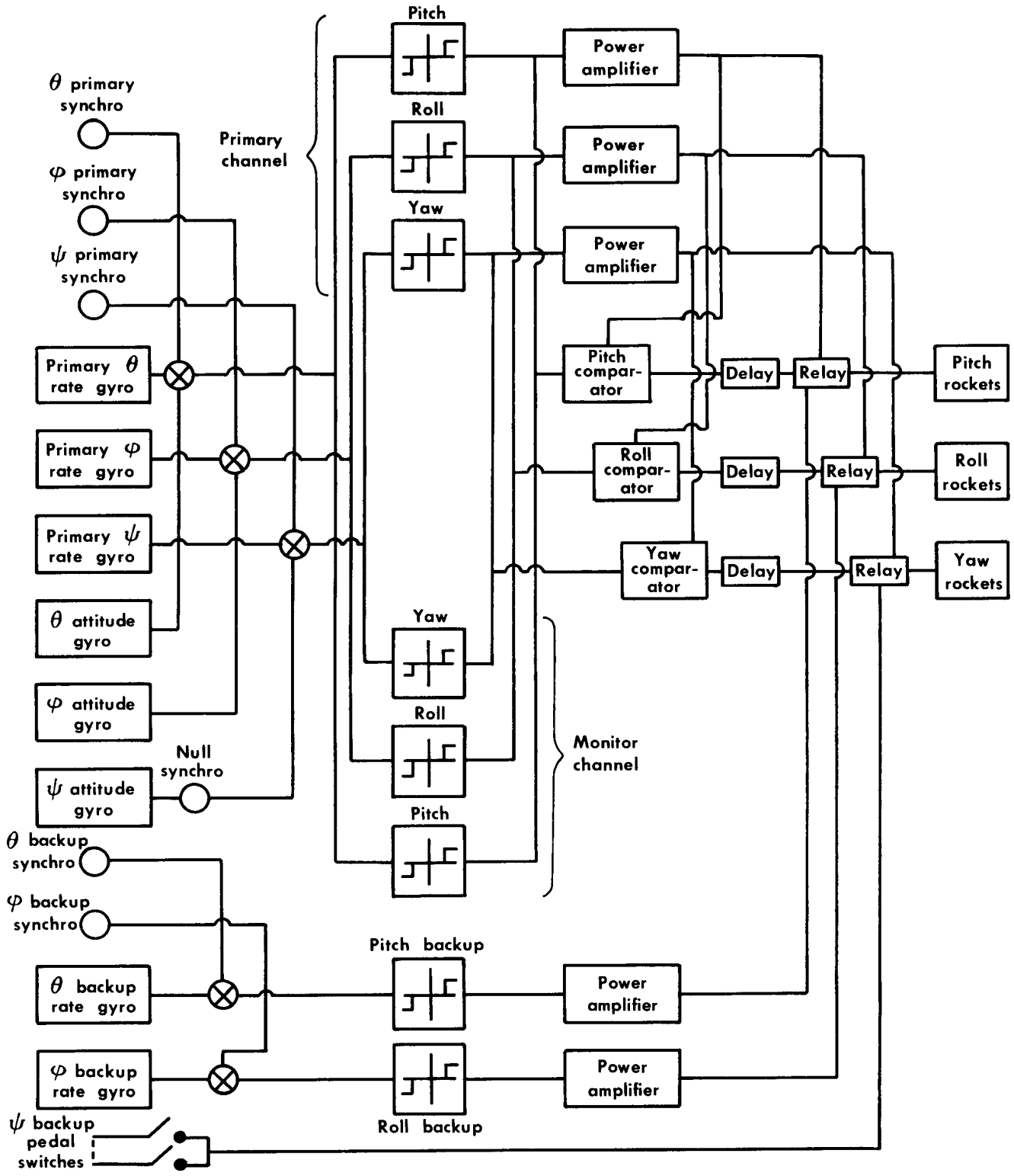

Figure 28.– Block diagram of primary and monitor circuitry of LLRV attitude control system.

Excessive Vehicle-Rate Detector

Since only one rate gyro is used for both the primary- and monitor-channel inputs of a given control axis, a hard-over failure in the gyro would not be detected by the comparator. For this reason, separate circuits are used to detect excessive outputs from the primary rate gyros. If the circuits checking the output of the primary pitch- and roll-rate gyros detect an excessive rate, they switch the pitch/roll channel into the backup mode. If the circuit checking the output of the primary yaw-rate gyro detects an excessive yaw rate, the yaw channel is switched into the backup mode. The vehicle rate at which transfer to the backup mode occurs is adjustable and is generally set for a 40 deg/sec (0.7 rad/sec) rate about each control axis, since this corresponds to the maximum rate-gyro output.

Roll-Authority Warning

Early in the design of the LLRV attitude control system, it was noticed that several factors contributed to reducing the roll control available to the pilot during a flight. The most significant contributors are uneven hydrogen-peroxide fuel consumption from the two side-mounted storage tanks, uneven lift-rocket thrust, jet-engine misalinement, and aerodynamic moments. Analysis indicated that these factors could result in a complete loss of roll-control power without the pilot being aware of the situation until the rate gyros could no longer counteract the roll-trim misalinement. For this reason, circuits were incorporated into the ACS monitor to determine the ratio of time that the roll-right rockets are on compared to the time the roll-left rockets are on. The pilot is then provided with an indication of unbalanced roll moments on the vehicle. Two indicator lights are available, one for excessive roll right and one for excessive roll left. The roll-authority circuitry illuminates the appropriate indicator light when the firing rate of the roll rockets in one direction exceeds the firing rate of the roll rockets in the opposite direction by a certain percentage over a preset period. The circuit is generally set so that a 50-percent loss in roll-control authority in either direction over an 8-second period will illuminate the appropriate indicator light.

Rocket-Valve-Stuck Circuitry

Although the ACS monitor circuitry reveals electrical failures in the driving signals of the on-off solenoid rocket valve, mechanical problems associated with the valves are not revealed. For this reason, stuck-open valve circuits are employed with attitude-rocket chamber-pressure transducers used as sensing elements to provide an indication to the pilot in the event a valve sticks open. A diagram of the stuck-valve-rocket logic is shown in figure 29. Basically, the circuits check for rocket combinations which should not occur, since they will occur only if one valve has failed in an open position. The rocket-chamber pressure-transducer outputs of appropriate rocket combinations are applied to AND gate networks. The Boolean expressions for the individual AND gate outputs are shown in figure 29. In the event an output from one of the AND gates occurs, this signal is used to illuminate a valve-stuck warning light on the pilot's instrument panel and corrective action is taken by the pilot.

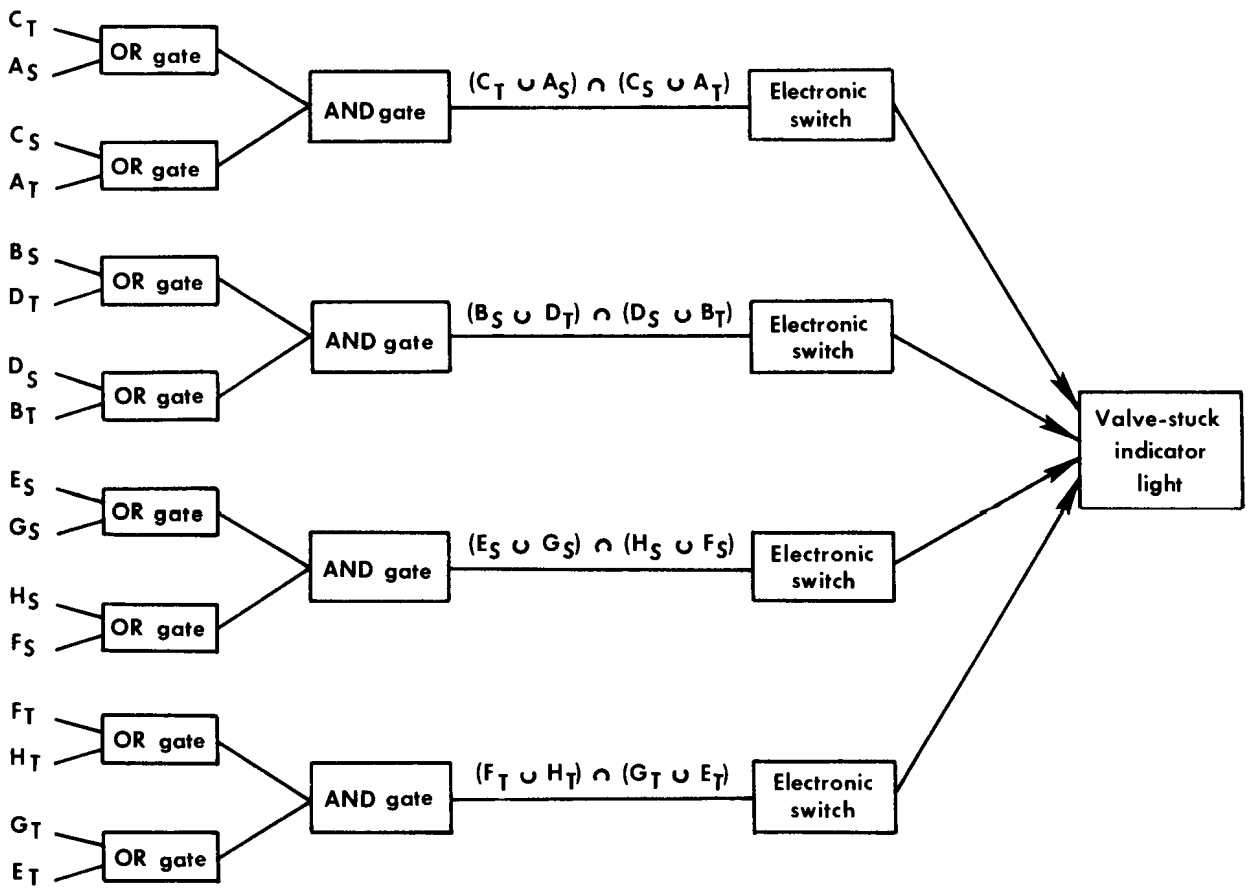

Figure 29.– Logic of stuck-rocket valve.

APPENDIX B

DETAILED DESCRIPTION OF THE LLRV JET-ENGINE ATTITUDE CONTROL SYSTEMS

A block diagram showing the components of the local-vertical and engine-centered systems is presented in figure 30. When operating in the local-vertical mode, the

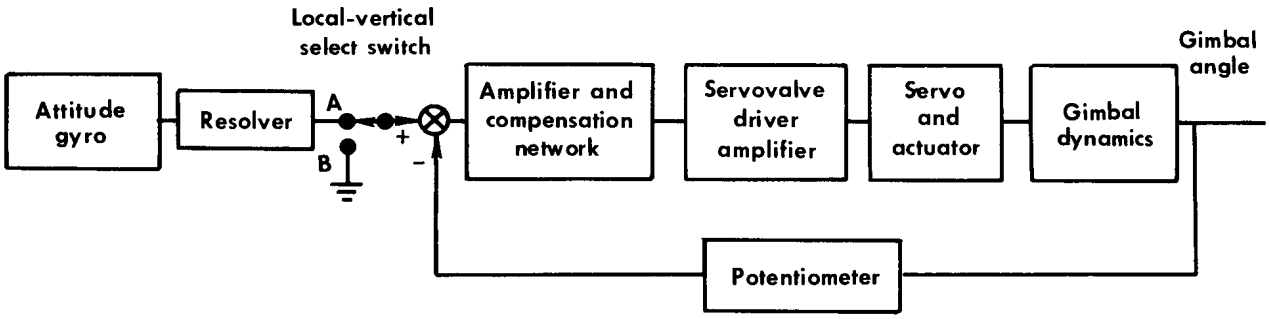

Figure 30.– Simplified block diagram of jet-engine attitude system, local-vertical and engine-centered modes.

switch is in position A and the input to the system is vehicle attitude. The attitude signals are obtained from attitude gyros employing synchro pickoffs. The earth-referenced attitude signal is then summed with a followup signal, which is proportional to the angle between the vehicle and the jet engine. The followup signal is obtained from a potentiometer which is mounted to sense relative angular motion between the jet engine and vehicle structure. The feedback signal is out of phase with the input signal so that an error signal results if the angle between the jet engine and the vehicle does not equal the attitude of the vehicle (gyro input to system). The error signal is then amplified and filtered and used to drive the hydraulic gimbal actuators to obtain the desired angle. The jet engine always remains vertical, therefore, relative to the earth. The angle between the engine and the vehicle is equal to the earth-referenced attitude of the vehicle.

In the engine-centered mode of operation, the switch shown in figure 30 is placed in position B, which removes the attitude-gyro input signal and grounds the input to the system. The feedback signal is always summed, then, with a zero input command signal resulting from the grounded input. The angle between the jet engine and the vehicle is therefore driven to zero and the engine remains alined with the vertical axis of the vehicle at all times.

The attitude limits of the jet engine when operating in the engine-centered mode are restricted to ±15° (±0.25 rad) from the vertical because of lubrication requirements. A special circuit is used which transfers the system from the engine-centered mode to the local-vertical mode in the event this 15° (0.25 rad) limitation is exceeded. If the transfer does not occur within 4 seconds, the emergency gimbal-locked mode is automatically selected. This additional safety feature prevents a transfer from being

made to the local-vertical mode from the engine-centered mode if a component failure common to both systems has occurred. Transfer to the emergency gimbal-locked mode from either the engine-centered or local-vertical mode also automatically occurs in the event of a normal dc or ac power failure.

APPENDIX C

DETAILED DESCRIPTION OF THE LLRV LUNAR-SIMULATION SYSTEM

Jet-Engine Stabilization System (JSS)

A simplified block diagram showing the components of the pitch axis of the jet-engine stabilization system is presented in figure 31. Identical components are used in the roll axis.

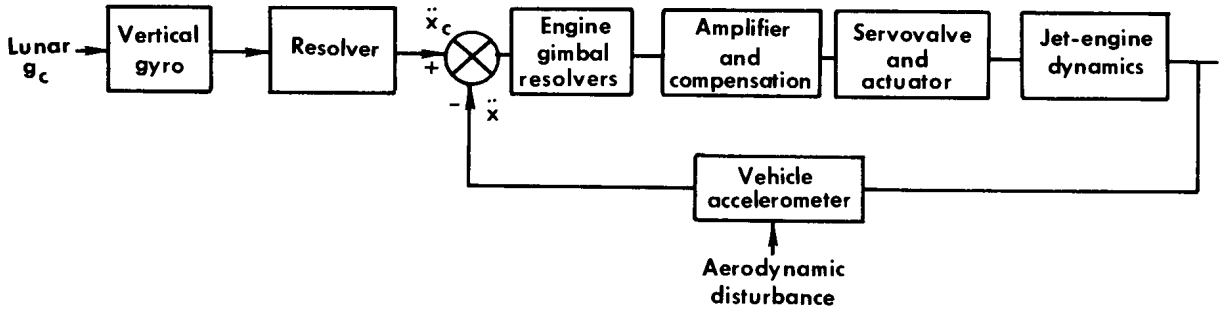

Figure 31.– Block diagram of lunar-gravity jet-engine stabilization system (pitch axis).

The g command input signal corresponds to an earth-referenced $\frac{5}{6}$ g acceleration. The command signal is resolved from an earth-referenced coordinate system to a body-axis coordinate system by means of vertical gyros which use resolver pickoffs. The output of the vertical resolver is a body-axis $\frac{5}{6}$ g command signal. The command signal for the pitch-axis case is compared with the $\ddot{x}$ acceleration of the vehicle, which is determined from body-mounted accelerometers. If a difference exists, an error signal results which is then resolved into a gimbal coordinate system by means of gimbal-mounted resolvers. The output of the gimbal-angle resolvers is then applied to an amplifier and compensation network. The resultant signal then drives the hydraulic servovalve and actuator assembly, causing the jet engine to tilt in a direction to correct for the acceleration error.

Since the accelerometers cannot be positioned at the vertical center of gravity, it is necessary to use two accelerometers for each translational acceleration required, i.e., $\ddot{x}$, $\ddot{y}$, and $\ddot{z}$. The locations of the accelerometers about the vehicle are shown in figure 32. The accelerometer pairs are mounted to the vehicle structural-ring assembly on either side of the jet engine. With this arrangement, centrifugal acceleration is automatically canceled by summing the accelerometer-pair outputs.

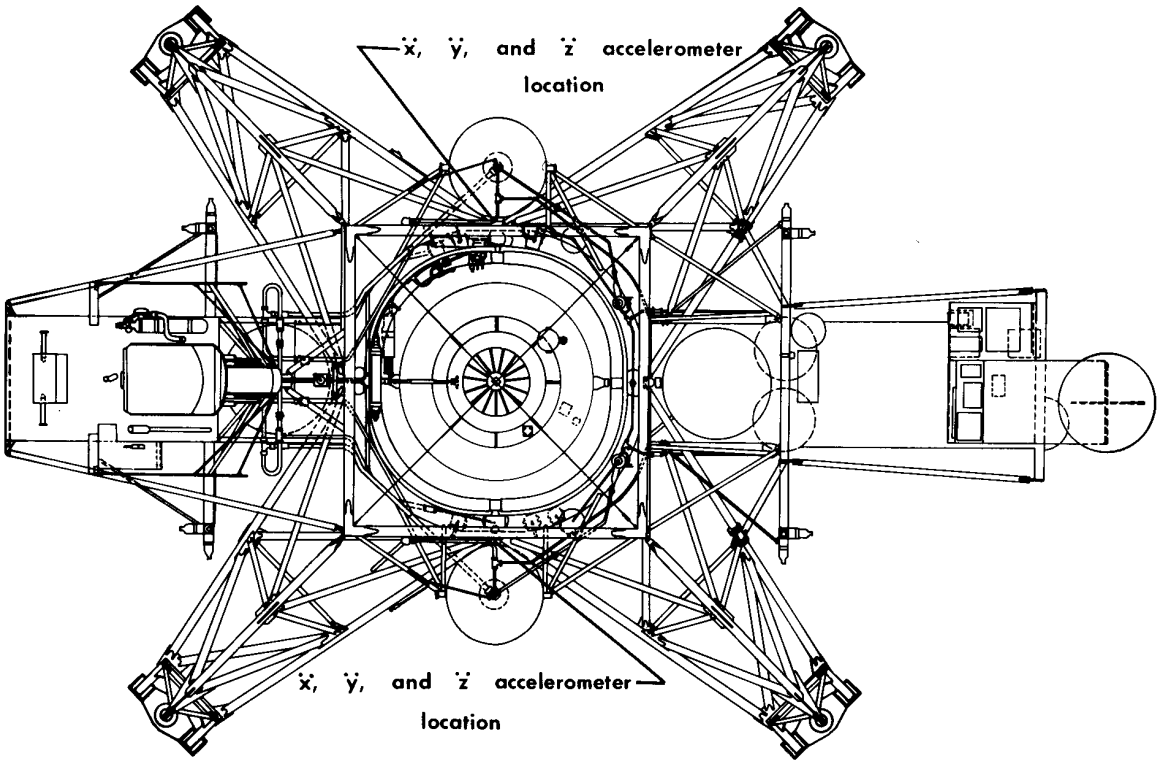

Figure 32.– Jet-stabilization-system accelerometer locations.

Automatic-Throttle System (ATS)

A simplified block diagram of the automatic-throttle system is presented in figure 33. The earth-referenced $\frac{5}{6}$ g command signal is resolved into body-axis coordinates as in the jet-engine stabilization system. The resultant signal is compared to the actual z-axis acceleration of the vehicle which is obtained from the body-mounted accelerometer (fig. 32).

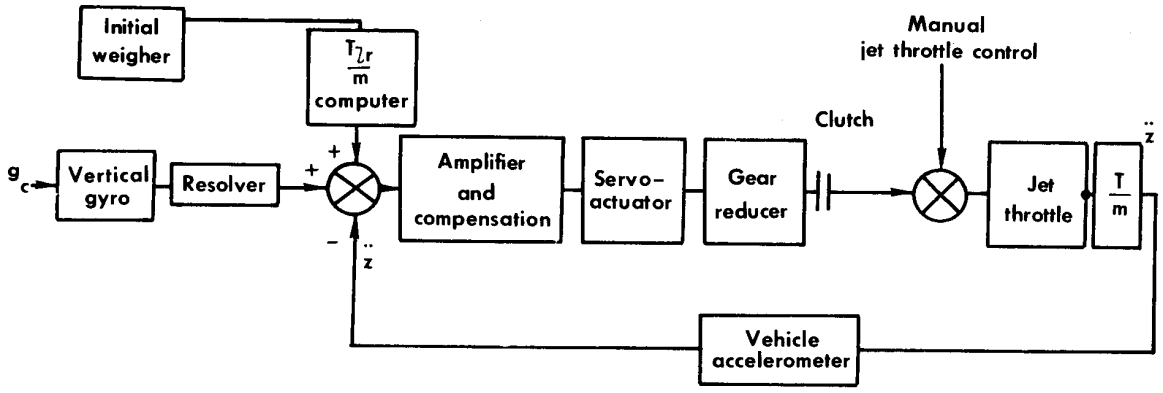

Figure 33.– Block diagram of lunar-gravity automatic-throttle system.

Since the vehicle accelerometers sense acceleration due to lift-rocket operation as well as jet-engine operation, a signal proportional to the acceleration commanded by the lift rockets must be included in the automatic-throttle loop. This signal is derived from a thrust-to-weight computer which computes the z-body-axis acceleration which should result from a given lift-rocket thrust. This signal is then summed with the $\frac{5}{6}$ g command signal and the $\dot{z}$-accelerometer feedback. The resultant error signal is then applied to an amplifier and compensation network used for stabilization. The output of this network then operates an electrical servoactuator and gear-reduction arrangement which positions the jet-engine throttle. A clutch assembly is located between the automatic-throttle actuator and jet-engine throttle and is energized only when the ATS is engaged. In the event a malfunction occurs in the ATS, the pilot can override the clutch with a 150 in.-lb (17 N-m) torque applied to the jet-throttle control.

Limit switches are also incorporated into the ATS to insure that the jet throttle does not exceed a preset maximum or minimum throttle position. A maximum limit switch is located at the 84° (1.47-rad) throttle position, and a minimum limit switch is located at the 78° (1.37-rad) throttle position. During ATS operation, if the maximum or minimum throttle position is attained, the input signal to the automatic-throttle actuator is opened, preventing further actuator movement. If a signal then occurs which would drive the throttle away from the limit, the input to the actuator is automatically applied, allowing the movement to take place. Another limit switch, designated as the low-thrust limit, is located at a throttle position below the minimum-limit switch. Should a malfunction occur in the circuitry of the minimum-limit switch and the minimum jet-throttle position actually be exceeded, the low-thrust switch is activated, which disengages the ATS clutch assembly and illuminates an indicator light on the pilot's instrument panel.

$\frac{T_{lr}}{W}$ Computer and Initial Weigher

A diagram showing the components and operation of the $\frac{T_{lr}}{W}$ computer is presented in figure 34. The purpose of the computer is to determine the actual acceleration commanded by lift-rocket operation so that this signal can be summed with the $\frac{5}{6}$ g command and followup signals at the input of the ATS. In order to accurately determine the acceleration of the vehicle due to lift-rocket thrust, it is first necessary to determine the weight of the vehicle. This is accomplished automatically by an initial weighing circuit which is composed of two integrators, a switching amplifier, and relay A, as shown in figure 34.

In normal operation, the pilot arms the initial weighing circuitry by applying power to the various components before firing the lift rockets. When the initial weighing circuit is armed and the lift-rocket throttle is off (no lift-rocket thrust), the microswitch on the lift-rocket handle and the Δg switch are in the positions shown in figure 34. The vehicle $\dot{z}$-accelerometer output is applied to the input of a nulling integrator. The output of this integrator is of proper sign and amplitude to drive the voltage at point ① to zero. A voltage proportional to some Δg (generally on the order of 0.1g) is obtained from the Δg potentiometer and applied to the arm of the Δg

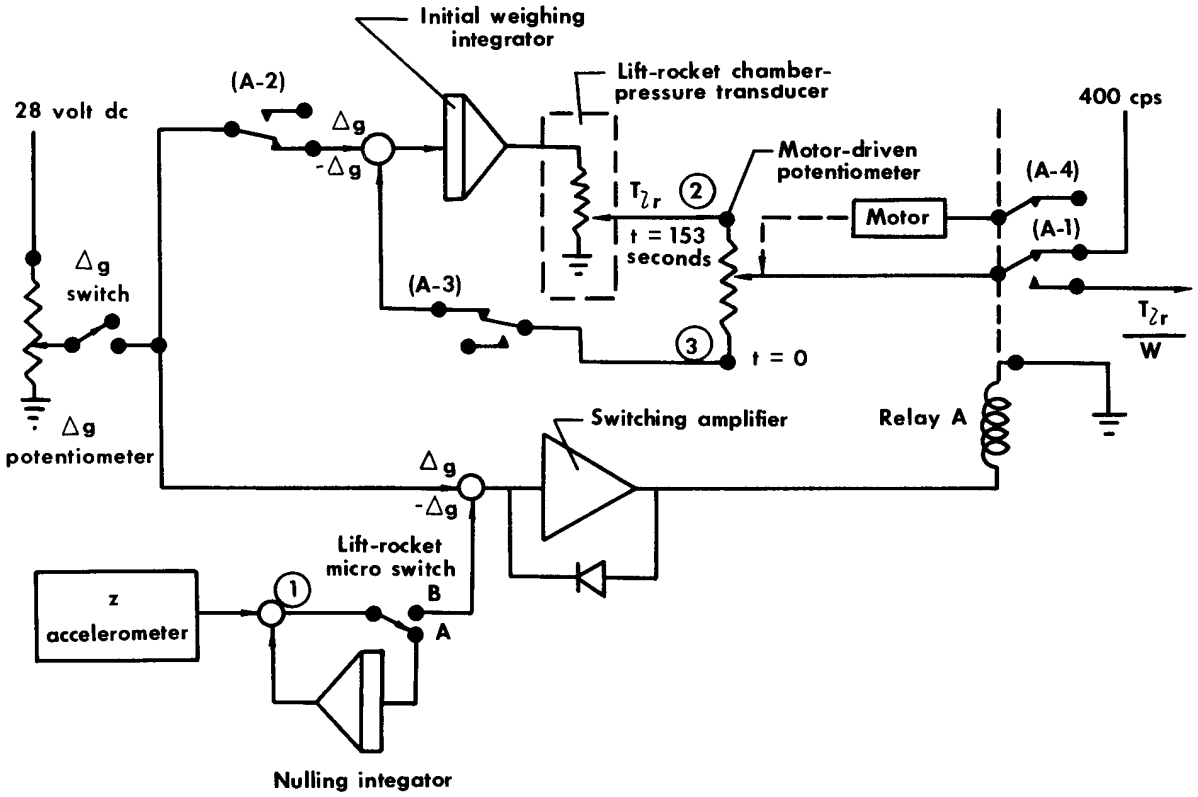

Figure 34.– Block diagram of $\frac{T_{lr}}{W}$ computer and initial weighing circuitry.

switch and to the input of the switching amplifier, biasing it off. The contacts of relay A are initially in the positions shown. The lift-rocket chamber-pressure-transducer output is zero, and the motor-driven potentiometer used to compensate for fuel burnoff is at the position which corresponds to t = 0 second.

The pilot starts the weighing action by lifting the rocket throttle and firing the lift rockets. At the instant the lift-rocket handle is moved, the microswitch on the lift-rocket handle and the Δg switch, which are connected directly to the handle, are transferred to the positions opposite those shown in figure 34. The input of the nulling integrator is now open, and the voltage at point ① begins to increase from zero as the 'z'-accelerometer output changes due to the lift-rocket thrust. The changing voltage at point ① , which is now proportional to the acceleration of the vehicle as a result of lift-rocket thrust only, is summed with the Δg voltage and applied to the input of the switching amplifier. The Δg voltage is also applied to the input of the initial weighing integrator through the Δg switch and relay contact A-2. The output of this integrator is applied as excitation to the lift-rocket chamber-pressure transducer. Since the lift rockets have been fired, a voltage now exists at point ② which is proportional to the product of the weighing integrator output and gain of the lift-rocket chamber-pressure transducer. The voltage at point ② is applied as excitation to the motor-driven fuel-burnoff potentiometer. The voltage at point ③ , which is the initial value

of the $\frac{T_{lr}}{W}$ computer $\left(\frac{T_{lr}}{W_i}\right)$, is fed back through relay contact A-3 and compared with the Δg input to the initial weighing integrator. The output of this integrator then changes until the initial $\frac{T_{lr}}{W_i}$ signal at point ③ is equivalent to the preset Δg voltage. It is important to note that the voltage at point ③ is independent of lift-rocket thrust. As the lift-rocket chamber-pressure transducer changes position corresponding to a change in lift-rocket thrust, the weighing-integrator output changes in a direction to keep the voltage at point ③ equivalent to the Δg voltage.

The pilot now continues to increase the lift-rocket thrust until the voltage at point ① is equivalent to a change in vehicle acceleration of Δg. At this point, the switching amplifier is fired and relay A is engaged. The initial voltage out of the computer is then proportional to $\frac{T_{lr}}{W_i}$ and is fed directly to the input of the ATS. The inputs to the weighing integrator are opened, and the excitation voltage to the lift-rocket chamber-pressure transducer is held constant. The motor that drives the fuel-burnoff potentiometer is also engaged by relay A. The potentiometer is scaled to compensate for a vehicle weight change of 300 lb/min (1335 N/min) due to hydrogen-peroxide and JP-4 fuel burnoff over a period of 153 seconds.

The vehicle-weighing action may be accomplished several times if necessary during a simulation flight. The pilot places the lift-rocket throttle in the off position and recycles the JSS switch on the left console, which deenergizes relay A. The steps necessary to accomplish the weighing maneuver can then be taken.

REFERENCES

1. Anon: Feasibility Study for a Lunar Landing Flight Research Vehicle. Rep. No. 7161-950001 (Contract NAS 4-174), Bell Aerosystems Co., Mar. 8, 1962.

2. Levin, Kenneth L.; and Decrevel, Roland: Problems of Earth Simulation of Manned Lunar Landing. Preprint No. 2691-62, ARS, Nov. 13-18, 1962.

3. Mechtly, E. A.: The International System of Units - Physical Constants and Conversion Factors. NASA SP-7012, 1964.

4. Bellman, Donald R.; and Matranga, Gene J.: Design and Operational Characteristics of a Lunar-Landing Research Vehicle. NASA TN D-3023, 1965.

5. Cooper, George E.: Understanding and Interpreting Pilot Opinion. Aeron. Eng. Rev., vol. 16, no. 3, Mar. 1957, pp. 47-51, 56.

TABLE I. – ACS PARAMETERS INVESTIGATED DURING FIRST 20 LLRV FLIGHTS

Flight number	Rate deadband, deg/sec (rad/sec)			Controller sensitivity, deg/sec per deg (rad/sec per rad)			Control authority, deg/sec^2 (rad/sec^2)			Flight objective
	Θ	φ	ψ	Θ	φ	ψ	Θ	φ	ψ	
1	1 (0.017)	1 (0.017)	2 (0.034)	3 (0.051)	3 (0.051)	1 (0.017)	32 (0.559)	46 (0.8)	15 (0.262)	Evaluation of local-vertical mode and ACS.
2	1 (.017)	1 (.017)	2 (.034)	3 (.051)	3 (.051)	1 (.017)	16 (.23)	23 (.4)	7.5 (.131)	Evaluation of local-vertical mode and ACS.
3	1 (.017)	1 (.017)	2 (.034)	3 (.051)	3 (.051)	1 (.017)	16 (.23)	23 (.4)	7.5 (.131)	Evaluation of local-vertical mode and ACS.
4	1 (.017)	1 (.017)	2 (.034)	3 (.051)	3 (.051)	1 (.017)	16 (.23)	23 (.4)	7.5 (.131)	Evaluation of gimbal-locked mode and ACS.
5	1.5 (.026)	1.5 (.026)	2 (.034)	3 (.051)	3 (.051)	1 (.017)	16 (.23)	23 (.4)	7.5 (.131)	Evaluation of lift rocket and ACS.
6	1.5 (.026)	1.5 (.026)	2 (.034)	3 (.051)	3 (.051)	1 (.017)	10.5 (.183)	14.5 (.254)	9 (.156)	Evaluation of lift rocket and ACS.
7	1.5 (.026)	1.5 (.026)	2 (.034)	3 (.051)	3 (.051)	1 (.017)	10.5 (.183)	14.5 (.254)	9 (.156)	Evaluation of lift rocket and ACS.
8	1.5 (.026)	1.5 (.026)	2 (.034)	3 (.051)	3 (.051)	1 (.017)	10.5 (.183)	14.5 (.254)	9 (.156)	Evaluation of lift rocket and ACS.
9	1.5 (.026)	1.5 (.026)	2 (.034)	3 (.051)	3 (.051)	1 (.017)	10.5 (.183)	14.5 (.254)	9 (.156)	Pilot familiarization.
10	1.5 (.026)	1.5 (.026)	2 (.034)	3 (.051)	3 (.051)	1 (.017)	10.5 (.183)	14.5 (.254)	9 (.156)	Pilot familiarization.
11	1.5 (.026)	1.5 (.026)	2 (.034)	3 (.051)	3 (.051)	1 (.017)	26.5 (.462)	37 (.644)	21.5 (.375)	Maintenance checkout.
12	2 (.034)	2 (.034)	2 (.034)	3 (.051)	3 (.051)	1.5 (.026)	16 (.23)	23 (.4)	7.5 (.131)	Evaluation of automatic-throttle system.
13	2 (.034)	2 (.034)	2 (.034)	3 (.051)	3 (.051)	1.5 (.026)	16 (.23)	23 (.4)	7.5 (.131)	Evaluation of automatic-throttle system and engine-centered mode.
14	2 (.034)	2 (.034)	2 (.034)	3 (.051)	3 (.051)	1.5 (.026)	16 (.23)	23 (.4)	7.5 (.131)	Evaluation of automatic-throttle system and jet-stabilization system.
15	2 (.034)	2 (.034)	2 (.034)	3 (.051)	3 (.051)	1.5 (.026)	16 (.23)	23 (.4)	7.5 (.131)	Evaluation of automatic-throttle system.
16	2 (.034)	2 (.034)	2 (.034)	3 (.051)	3 (.051)	1.5 (.026)	16 (.23)	23 (.4)	7.5 (.131)	Evaluation of automatic-throttle system.
17	2 (.034)	2 (.034)	2 (.034)	3 (.051)	3 (.051)	1.5 (.026)	16 (.23)	23 (.4)	7.5 (.131)	Evaluation of automatic-throttle system and jet-stabilization system.
18	2 (.034)	2 (.034)	2 (.034)	3 (.051)	3 (.051)	1.5 (.026)	16 (.23)	23 (.4)	7.5 (.131)	Evaluation of automatic-throttle system and jet-stabilization system.
19	2 (.034)	2 (.034)	2 (.034)	3 (.051)	3 (.051)	1.5 (.026)	16 (.23)	23 (.4)	7.5 (.131)	Evaluation of automatic-throttle system and jet-stabilization system.
20	2 (.034)	2 (.034)	2 (.034)	3 (.051)	3 (.051)	1.5 (.026)	16 (.23)	23 (.4)	7.5 (.131)	Evaluation of automatic-throttle system and jet-stabilization system.

TABLE II. – FAILURE HISTORY OF LLRV AVIONICS

Date	Operation	Description of malfunction
5/64	Ground test	Broken wire on relay in electrical system.
5/64	Ground test	Cut wire bundle resulting from improper clamp installation.
8/64	Preflight	Primary 400-cycle ac inverter failure. Overheating resulted from covering being placed over the inverter to protect from rain. Field winding burned open.
8/64	Ground test	Emergency 28-volt dc battery failure. Failure was the result of a design discrepancy which caused continuous battery drain even though emergency power was not being used.
8/64	Ground test	Broken wire resulting from flexure at roll-gimbal point.
8/64	Ground test	Transformer failed in weight and drag computer.
9/64	Ground test	Broken lead on rate gyro.
9/64	Ground test	Vertical gyro with synchro output failed during bench calibration. Spin motor winding burned open as a result of the bearings seizing.
9/64	Ground test	Power transformer failed in gyro package due to wiring error.
10/64	Preflight	Intermittent terminal connection in yaw comparator circuitry.
10/64	Flight number 1	Intermittent terminal connection resulting in ACS failure to pitch/roll backup electronics.
11/64	Flight number 2	Intermittent terminal connection resulting in ACS failure to pitch/roll backup electronics.
11/64	Ground test	Intermittent terminal connection in yaw-monitor circuitry.
11/64	Flight number 3	Intermittent terminal connection resulting in ACS failure to pitch/roll backup electronics.
11/64	Preflight	Intermittent terminal connection in yaw input and summation circuitry.
11/64	Preflight	Intermittent terminal connection in pitch/roll input and summation circuitry.
11/64	Flight number 4	No malfunctions.
11/64	Flight number 5	Intermittent terminal connection resulting in ACS failure to yaw backup electronics.
11/64	Flight number 6	No malfunctions.
11/64	Flight number 7	No malfunctions.
12/64	Ground test	Broken wire on printed circuit-board terminal in monitor box.
12/64	Preflight	Failure of emergency 28-volt dc power relay due to short circuit.
12/64	Flight number 8	Intermittent terminal connection resulting in ACS failure to backup electronics.
12/64	Flight number 9	No malfunctions.
12/64	Flight number 10	No malfunctions.
1/65	Ground test	Failure of vertical gyro with resolver output. Open spin motor winding.
1/65	Ground test	Failure of vertical gyro with synchro output. Gyro would not transfer to slow erection mode. (Heavyweight electronic boxes installed 1/65)
1/65	Ground test	Intermittent terminal connection in yaw-monitor circuitry.
2/65	Flight number 11	No malfunctions.
2/65	Preflight	Leg microswitch inoperative due to incorrect wiring.
2/65	Flight number 12	No malfunctions.
3/65	Flight number 13	No malfunctions.
3/65	Ground test	Failure of 400-cps demodulator filter in weight and drag computer.
3/65	Preflight	Emergency 28-volt dc battery failure.
3/65	Flight number 14	No malfunctions.
3/65	Flight number 15	No malfunctions.
4/65	Ground test	Broken wire on primary roll-rate gyro input to ACS circuitry.
4/65	Ground test	Gear assembly in automatic-throttle actuator failed due to excessive wear.
4/65	Preflight	Primary roll-rate gyro failed to meet minimum spin-rate requirements.
4/65	Flight number 16	No malfunctions.
4/65	Flight number 17	No malfunctions.
5/65	Flight number 18	Lift-rocket chamber-pressure transducer used in weight and drag computation failed.
5/65	Ground test	Failure of dc amplifier in weight and drag computer.
5/65	Flight number 19	No malfunctions.
5/65	Flight number 20	No malfunctions.
6/65	Ground test	Diode failure in weight and drag computer.
6/65	Ground test	Vertical gyro with resolver output. Null-point shift.